

22NRM02 STANBC



D1: Calibration guide

Guide on the traceable calibration of in situ EMS and PTI methods to determine aerosol light absorption coefficients as a function of the light source wavelength and aerosol SSA using reference gases and aerosols with an uncertainty budget (target ≤10 %)

Organisation name of the lead participant for the deliverable: Jozef Stefan Institute

Due date of the deliverable:

31.5.2024

Actual submission date of the deliverable:

17.3.2025

Confidentiality Status: SEN – Sensitive, limited under the conditions of the Grant Agreement

Deliverable D1

Funded by the European Union. Views and opinions expressed are however those of the author(s) only and do not necessarily reflect those of the European Union or EURAMET. Neither the European Union nor the granting authority can be held responsible for them.

METROLOGY PARTNERSHIP

European Partnership



Co-funded by the European Union



Glossary

PTAAM Photo-thermal aerosol absorption monitor

PTI Photo-thermal interferometry

TMPG Traceable mobile permeation generator

IR Infrared

DMA Differential mobility analyser
Dp electrical mobility diameter

CPMA Centrifugal particle mass analyser

D_m mass equivalent diameterEMS Extinction minus scatteringCAPS Cavity attenuated phase shift

FCAE Faraday cup aerosol electrometer

22NRM02 STANBC



TABLE OF CONTENTS

1 Summary	4
2 Traceable calibration of photo thermal aerosol absorption monitor	(PTAAM) 5
2.1 Traceable calibration with absorbing gases	`5
2.1.1 NO2 absorption spectrum	
2.1.2 Pump laser emission spectrum	
2.1.3 Traceable generation of NO ₂	6
2.1.4 Secondary standard – CAPS NO ₂ monitor	6
2.1.5. Premixed samples	
2.1.6 Calibration with ambient NO2	
2.1.7 Uncertainty analysis for calibration with NO ₂	
2.2 Traceable calibration with absorbing particles	
2.2.1 Nigrosin refractive index	
2.2.2 Shape and effective density of the particles	
2.2.3 Hybrid gas & polydisperse nigrosin particle calibration of infrared of	
2.2.3 Monodisperse nigrosin particles selected with a differential mobilit	
2.2.4 Monodisperse nigrosin particles selected with a centrifugal particle	
2.2.5 Monodisperse nigrosin particles selected with tandem CPMA and I	
2.3 Uncertainty analysis	
3 Traceable calibration of extinction-minus-scattering (EMS)	
3.1 Measurement setup	
3.2 Calibration	
3.3 Noise	16
3.4 Repeatability of calibration factors	
3.5 Uncertainty in the determination of the gas absorption coefficient	nts 17
3.6 SI-traceability	
4 References	
5 Supplemental material	



1 Summary

Traceable calibration procedures for photo-thermal aerosol absorption monitor (PTAAM) based on absorbing NO₂ gas and nigrosin particles were developed. NO₂ calibration uses a traceable mobile permeation generator (TMPG) to produce NO₂ with a precise mixing ratio in the carrier gas. Gas absorption is calculated from the overlap of high resolution NO₂ absorption spectrum with the emission spectrum of measurement light source. Calibration with nigrosin particles is based on known refractive index and the selected size of monodisperse particles. Particle size selection using centrifugal particle mass analyzer and electrostatic classifier in series is proposed. Mie calculation is then performed using mass equivalent diameter and measured particle number concentration to produce absorption coefficient at the desired wavelength. Nigrosin enables calibration in the whole visible and near infrared spectrum while NO₂ calibration is limited to the visible part.

The sources of PTAAM uncertainty depend on the wavelength under investigation and not all listed apply to all wavelengths or to all listed calibration protocols. The uncertainty includes the reproducibility of the PTAAM measurement. These sources are: NO₂ amount fraction; NO₂ absorption cross-section; Mie calculation and nigrosin refractive index; Mie calculation and particle size distribution; scattering and absorbing gasses; stability of PTAAM response; measurement uncertainty of particle counting instruments; multiple charge correction; uncertainty of size/mass selection instrumentation.

The uncertainty of calibration with NO₂ (k=2, 95% confidence interval) is 8.4%. For calibration using monodisperse nigrosin particles selected by the tandem CPMA + DMA we obtained the uncertainty of 9.6%.

Extinction minus scattering (EMS) as a traceable system for reference absorbance was investigated in detail as part of the EMPIR black carbon project. The system was a three-wavelength system consisting of an Aurora 4000 nephelometer and three CAPS_{pmex} monitors. The system was also used for the *stanBC* laboratory studies. Traceability was established by calibrating the nephelometer with a gas of known Rayleigh scattering coefficient. In a second step, the extinction cell is calibrated by comparing light extinction and light scattering for non-absorbing aerosol particles.

The sources of EMS uncertainty are related to both measurements – scattering and extinction. The stated uncertainty does not include the repeatability of the EMS measurement. These sources are: CO2 amount fraction; CO2 scattering cross-section (not included yet); repeatability of CO2 calibration; systematic error of CO2 calibration; stability of composition of zero-air; nephelometer noise; CAPS_{pmex} noise; nephelometer truncation error; error of calibration constants of the nephelometer; CAPS_{pmex} calibration error (effective light path length); CAPS calibration repeatability; CAPS_{pmex} baseline drift.

The closer the absorbance and scattering values are to each other, the greater the uncertainty in the derived light absorption. Uncertainties due to noise and baseline drift can be effectively reduced by long averaging times with repeated baseline measurements. However, long averaging times cannot reduce the high uncertainties associated with low concentrations and less absorbing particles. For highly absorbing particles such as soot, for example, the relative uncertainty can be as low as 3 % (k=2), while it increases dramatically at low concentrations (extinction coefficient below 10 1/Mm). For single scattering albedos (SSA) of more than 0.8, the uncertainty is more than 10 % and even increases strongly at low concentrations (extinction coefficient below 20 1/Mm).



2 Traceable calibration of photo thermal aerosol absorption monitor (PTAAM)

2.1 Traceable calibration with absorbing gases

Traceable calibration is done with mixture of NO2 and synthetic air. Calibration is based on:

- absorption spectrum of NO2
- emission spectrum of pump laser
- NO₂ mixing ratio in calibration sample
- correction for NO2 losses in the instrument

2.1.1 NO2 absorption spectrum

The NO₂ absorption spectrum has fine structure (Figure 1) which depends on pressure and temperature. High resolution (0.25 nm) absorption spectra from Vandaele et al. (2002) and Bogumil et al. (2003) were downloaded from a spectral atlas (https://www.uv-vis-spectral-atlas-mainz.org, Keller-Rudek et al., 2013).

 NO_2 allows for calibration of the 450 nm channel; at 808 nm the absorption of NO_2 is too low for calibration. The IR channel of the PTAAM is thus calibrated by comparison to 450 nm using a Mie-calculated absorption ratio $b_{abs}(808 \text{ nm})/b_{abs}(450 \text{ nm})$ for polydisperse nigrosin particles (Drinovec et al., 2022).

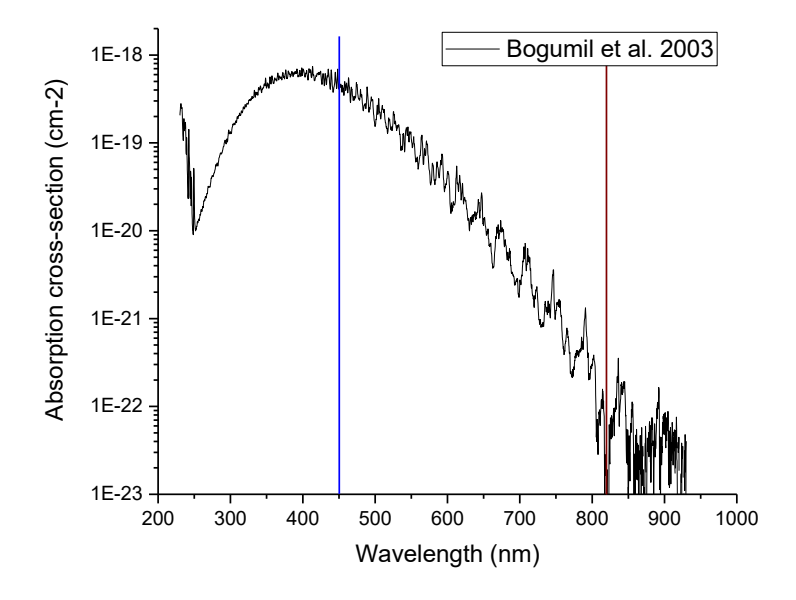


Figure 1. Absorption spectrum of NO₂



2.1.2 Pump laser emission spectrum

Due to the fine structure of NO_2 absorption it is essential to measure emission spectrum of the pump laser and calculate the corresponding absorption cross section (Arnott et al., 2000; Schnaiter et al., 2023). To measure the laser spectrum a high-resolution spectrometer (spectral accuracy < 1 nm) is needed. Portable spectrometers need to be calibrated before the measurement due to mechanical and temperature drifts. A calibration lamp with neon emission lines (Thorlabs CSL1) was used for spectrometer calibration. An example of a pump laser spectra and the absorption cross section of NO_2 is shown on Figure 2.

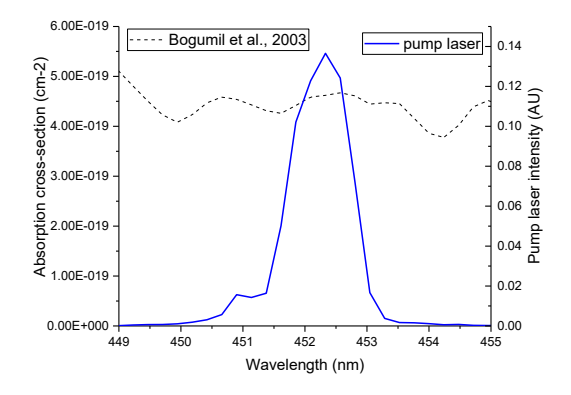


Figure 2. Absorption cross section of NO2 at 293 K and emission spectrum of PTAAM's pump laser

2.1.3 Traceable generation of NO₂

A permeator is a device which emits NO₂ through a permeable membrane. The amount of released NO₂ is measured in a levitation chamber, then the permeator is installed in the mobile generator. A traceable mobile permeation generator (TMPG) developed by METAS (Haerri et al., 2017) produced 292 nmol/mol of NO₂ in synthetic air which was used for calibration of PTAAM (Drinovec et al. 2022).

2.1.4 Secondary standard – CAPS NO₂ monitor

If a TMPG is not available, then the NO_2 amount fraction in the calibration sample needs to be measured using a secondary measurement standard which has been traceably calibrated. In this study, we tested a CAPS NO_2 monitor (Aerodyne, USA). The instrument was initially calibrated by the manufacturer using an Ecotech Serinus calibrator, which generates a known amount of NO_2 by reacting an excess of NO (~100 ppm in nitrogen) with ozone from a NIST-calibrated ozone source. The CAPS NO_2 monitor agreed within 1% with the TMPG. The secondary standard is then used to measure NO_2 concentration in a NO_2 sample which is used for calibration.



2.1.5. Premixed samples

Due to the limited upper range of absorption instruments a NO_2 sample in sub-ppm concentration is used. NO_2 mixed with the synthetic air (grade 5.5) can be purchased in pressurized cylinders. Our observations (Drinovec et al., 2022) show that bottled NO_2 concentration can differ for more than 20% from the nominal concentration of 1 ppm. For 10 ppm NO_2 bottles an initial decrease of NO_2 concentration up to 5% has been observed (Flores et al., 2021).

Since NO_2 is not completely chemically inert and can react, it is recommended that the NO_2 source is installed in short connections with not too low flow rates, so that the residence time in the transfer tubes is reduced to a minimum. it is also advantageous to use non-reactive tube materials such as Teflon.

2.1.6 Calibration with ambient NO₂

In urban environments it is possible to use ambient air as a source of NO₂. A NO₂ scrubber is used to produce a sample without NO₂ for the zero measurement. NO₂ concentration is measured using NO₂ monitor. A calibration experiment was conducted in Granada (Spain). The response agrees within 5% with the laboratory calibration (Figure 3).

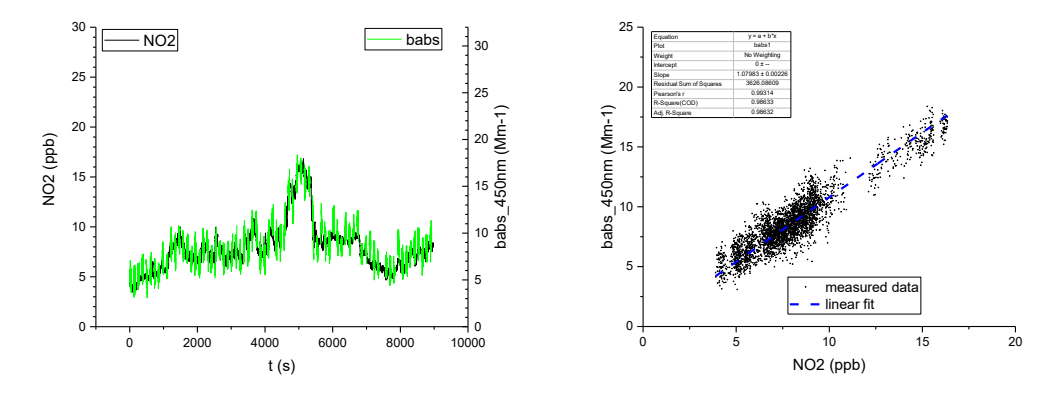


Figure 3. Comparison between ambient NO2 concentration and absorption at 450 nm.



2.2 Traceable calibration with absorbing particles

Traceable calibration with particles is based on the refractive index of the aerosol material, aerosol size/mass, shape and number concentration. Absorption coefficient is calculated using Mie theory (Mie, 1908) and available codes from Mätzler (2002) and Prahl (2007). For low uncertainty a monodisperse aerosol should be used.

Spherical particles can be produced by nebulizing a water-soluble substance. We have selected nigrosin (Acid black 2, Nigrosin water soluble, CAS 8005-03-6) which absorbs in visible and IR spectral regions.

2.2.1 Nigrosin refractive index

Nigrosin's refractive index was measured on thin film produced by slow drying of nigrosin dissolved in water (Drinovec et al., 2022). The imaginary part was measured using a spectrometer with integrating sphere. The real part of the refractive index was determined by measuring the Brewster angle. Measured values are presented in Table 1. The imaginary part of the refractive index is 14% lower compared to Bluvstein et al. (2017) nigrosin sample.

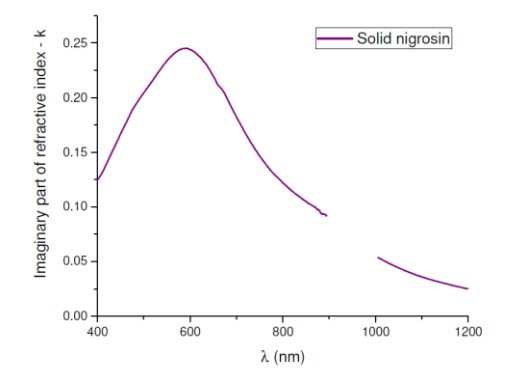


Figure 4. Imaginary part of the refractive index of solid nigrosin

Table 1. Measured values of nigrosin refractive index (Drinovec et al., 2022).

Wavelength (nm)	Refractive index	
450	1.58 + i0.167	_
532	1.62 + i0.223	
633	1.75 + i0.231	
808	1.78 + i0.119	
1064	1.73 + i0.0419	



2.2.2 Shape and effective density of the particles

For perfectly spherical particles it is possible to calculate the absorption cross section based on the wavelength of the light source, particle diameter and refractive index. If particle shape deviates from perfect sphere, then it becomes important how the particle diameter is measured. We have compared mobility diameter D_p measured using SMPS with mass-equivalent diameter D_m derived from particle mass measured by CPMA and using a nigrosin density of 1.6 g/cm3 (Moteki et al, 2010; Vokes et al., 2022).

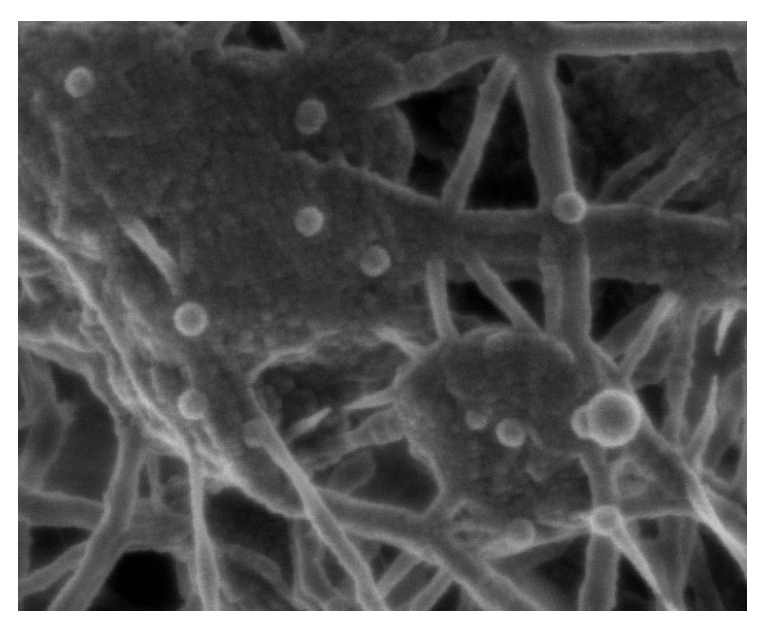


Figure 5. SEM image of nigrosin particles on filter.

An experiment was conducted by first selecting the mass of the particles using CPMA and then measuring mobility diameter using SMPS (Figure 6). Effective particle density increases with the particle mass/size (Table 2). We have obtained different densities at different nebulizer settings which indicate that the particle generation process is responsible for the variation. We have conducted a control experiment with polystyrene beads, where measured density equals that of polystyrene showing that CPMA and SMPS operate correctly.

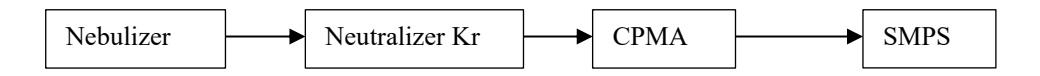


Figure 6. Measurement setup for determination of nigrosin particle effective density

Table 2. Comparison between mobility diameter D_p and mass equivalent diameter D_m for one of the experiments using nigrosin solution N2 (0.1 g/l)

m (fg)	D _p (nm)	D _m (nm)	Effective density (g/cm3)
1	111.4	106.1	1.38
3	158.7	153.0	1.43
10	233.7	228.5	1.50



2.2.3 Hybrid gas & polydisperse nigrosin particle calibration of infrared channel

The infrared channel cannot be calibrated using NO₂. For field calibration, when it is not possible to produce monodisperse nigrosin, a hybrid calibration method was developed (Drinovec et al., 2022). Hybrid calibration consists of:

- calibration of the 450 nm channel using NO₂,
- transferring calibration from 450 nm to the 808 nm channel using Mie calculated absorption ratio babs(808 nm)/babs(450 nm) for polydisperse nigrosin particles.

The absorption ratio has low aerosol diameter dependence in the nigrosin with mobility diameter below 250 nm (Figure 7). When using a nigrosin solution N2 (0.1 g/l) we obtain a volume distribution with the volume distribution peak at 109 nm (Figure 7). Here the polydisperse nigrosin absorption ratio babs(808 nm)/babs(450 nm) is 0.3344.

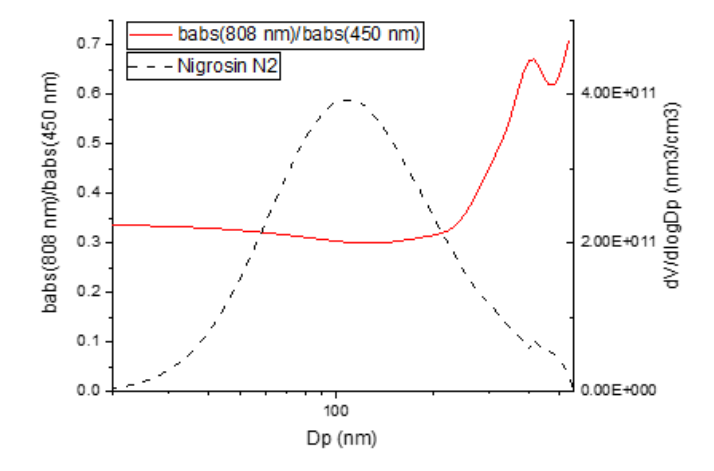


Figure 7. Size dependent Mie calculated absorption ratio for nigrosin and a polydisperse nigrosin volume size distribution used for calibration.



2.2.3 Monodisperse nigrosin particles selected with a differential mobility analyzer (DMA)

The particles are selected using an electrostatic classifier (DMA) set to fixed voltage and counted with CPC (Figure 8). Multiply charged particles of larger diameter but with the same electrical mobility are also transmitted. Their fraction was analyzed with CPMA-FCAE connected to DMA instead of CPC. The fraction of multiply charged particles can be reduced by selecting particles on the right side of the volume size distribution (Figure 9). Anyway, the data needs to be corrected for multiply charged particles.

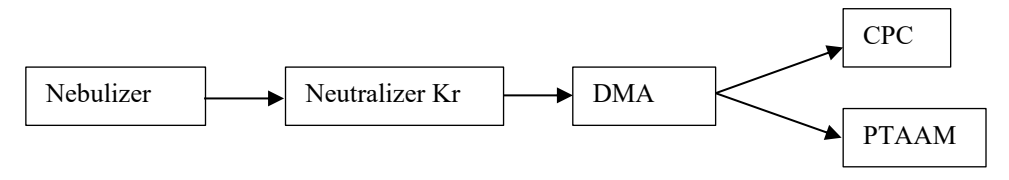


Figure 8. Particle size selection by differential mobility analyzer (DMA).

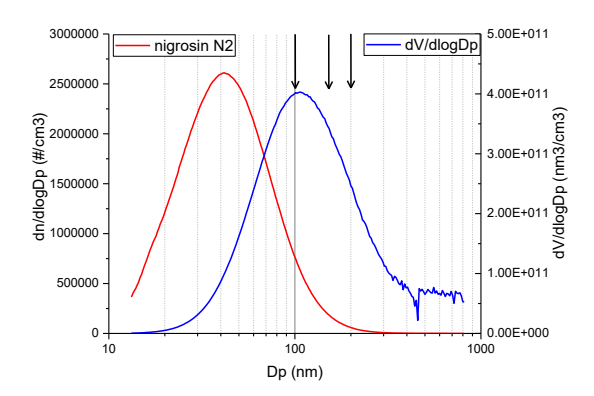


Figure 9. Particle size distribution generated by nebulizing nigrosin solution N3 (1 g/l). Arrows shows the selected mobility diameters.



2.2.4 Monodisperse nigrosin particles selected with a centrifugal particle mass analyzer (CPMA)

A CPMA was used to select particles with a mass of 1 fg (Figure 10). Neutral particles are not counted by Faraday cup aerosol electrometer (FCAE) but they can contribute to absorption. The number of transmitted neutral particles depends on the CPMA rotational speed – at higher speed (bigger value of Rm) fewer neutral particles are transmitted. The number of neutral particles can be further reduced by selecting the particle size on the left side of the volume distribution peak (Figure 11). Table 3 shows number concentrations measured using a CPC, which measures all particles including the neutral ones, and FCAE, which only measures charged particles. Table 3 shows the influence of Rm on the number of transmitted neutrals and their effect on absorption.

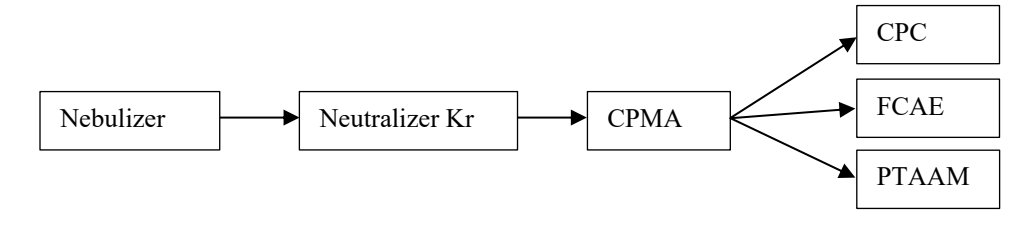


Figure 10. Particle mass selection using a centrifugal particle mass analyzer (CPMA).

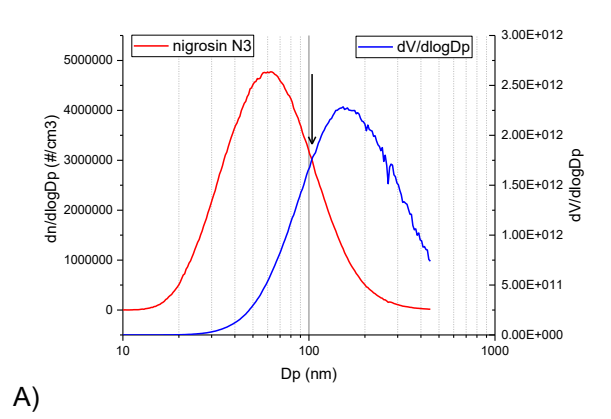


Figure 11. Particle size distribution generated by nebulizing nigrosin solution N3 (1 g/l). Arrow shows the selected mobility diameter (A)

Table 3. Comparison of particle number concentration as measured by a condensation particle counter (CPC) and an aerosol electrometer (FCAE). Mie calculation is based on FCAE and selected particle mass.

Rm	CPC	FCAE	Babs_PTAAM_450nm	Babs_Mie_450nm
	(#/cm3)	(#/cm3)	(Mm-1)	(Mm-1)
15	4362	3432	9.45	9.00
3	85889	20942	60.8	54.94



2.2.5 Monodisperse nigrosin particles selected with tandem CPMA and DMA

This method takes advantage of using two classifiers with different artifacts that cancel out to produce purely monodisperse particles, which can be counted using a CPC (Figure 12). For each particle mass (selected by CPMA) DMA voltage need to be set to the maximum of the particle size distribution. Both neutral particles and multiply charged particles are filtered out. Mie calculation of absorption for the selected particles is then based on mass equivalent diameter D_m .

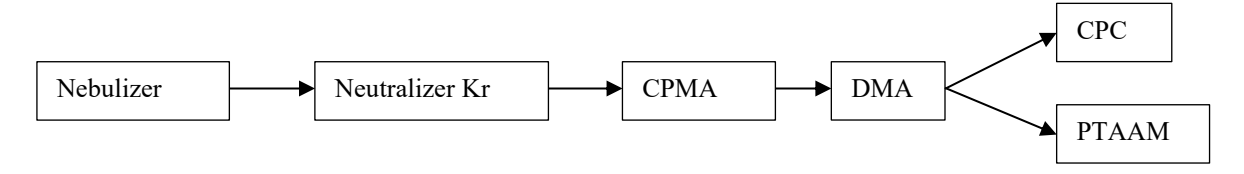


Figure 12. Particle size selection using a tandem centrifugal particle mass analyzer (CPMA) and differential mobility analyzer (DMA).



2.3 Uncertainty analysis

The uncertainty for determination of the absorption coefficient measured with PTAAM-2λ results from the calibration, method and instrumental uncertainties (Table 4) derived from Drinovec et al. (2022). The uncertainty budget was updated in Yus-Diez et al. (2025) with the addition of NO2 absorption cross-section uncertainty. The calibration of the 450 nm channel depends strongly on the uncertainty of NO2 amount fraction in the calibrating gas mixture. For NO2 mixtue produced by TMPG the standard uncertainty of NO2 amount fraction was below 2%. The calibration of the 808 nm channel depends on both the uncertainty of the 450 nm channel and the uncertainty of the calculated nigrosin absorption ratio babs(808 nm)/babs(450 nm); this parameter depends on the correct determination of nigrosin's refractive index and the measured size distribution. The uncertainties of the real part of the refractive index (2%) and of the imaginary part (3%) result in a 2% uncertainty of the absorption coefficient (coverage factor k=1, 68 % confidence interval). For wellserviced SMPS instruments, the uncertainty of dN/dlogDp in size bin is below 10% (Wiedensohler et al., 2017) The uncertainty of the ratio of the absorption coefficients is lower, estimated at 4%. Instrument operation can be influenced by the scattering artefact and the presence of absorbing gases. The absorption of gases is subtracted by measurement of filtered air, but a small amount of the gas can be adsorbed onto the filter material. The combined uncertainty of scattering and gases was estimated to be 1%. Finally, an uncertainty contribution comes from the stability of the instrument response (3%). For CPC the uncertainty depends on calibration and flow measurement resulting in 3% uncertainty (Wiedensohler et al., 2017). Due to high noise at low sample flow, we used 4% uncertainty for the FCAE. When using DMA for size selection the multiple charged particles contribute to about 20% of absorption. The exact quantification of multiple charged particles depends on multiple peak fitting and results is 5% uncertainty of the calculated absorption after correction. Combined standard uncertainties for the determination of absorption coefficients and absorption Ångström exponent are presented in the lower part of Table 4. The 808 nm channel uncertainty (6.2%) is higher compared to that of the 450 nm channel (4.2%) due to the additional calibration step with polydisperse nigrosin particles. The uncertainties for Mie calculated absorption coefficient of monodisperse nigrosin depend mostly on CPC and FCAE uncertainties. When using DMA for particle size selection, the uncertainty increases because of multiple charge correction.

Table 4. The sources of uncertainty and combined standard uncertainties (k = 1) of absorption coefficient for PTAAM traceably calibrated with gas and particles. Combined uncertainties were calculated using independent uncertainty components.

Source of uncertainty	Contributions	Uncertainty k=1	Uncertainty k=2, SSA<0.9
A: NO ₂ amount fraction		2%	
B: Absorption cross-section of NO ₂		2%	
C: Mie calculation & nigrosin refractive index		2%	
D: Mie calculation & particle size distribution:		4%	
E: Scattering and absorbing gasses		1%	
F: Stability of PTAAM response		3%	
G: CPC measurement uncertainty		3%	
H: FCAE measurement uncertainty		4%	
I: multiple charge correction		5%	
Combined uncertainties			
PTAAM 450 nm: calibration with NO ₂	A, B, E, F	4.2%	8.4%
PTAAM 808 nm: NO2 + polydisperse nigrosin	A, C, D, E, F	6.2%	12.4%
Monodisperse nigrosin - DMA	C, E, F, G, I	6.9%	13.9%
Monodisperse nigrosin – CPMA	C, E, F, H	5.5%	11%
Monodisperse nigrosin - CPMA + DMA	C, E, F, G	4.8%	9.6%



3 Traceable calibration of extinction-minus-scattering (EMS)

3.1 Measurement setup

The principle of Extinction minus Scattering (EMS) is to derive the light absorption from the difference between the measured light extinction and light scattering. The setup used in in this study consists of a three-wavelength integrating nephelometer Aurora4000 (Ecotech Pty LTD , Australia) and three CAPS_{pmex} (Aerodyne Research, Inc., USA) devices. The wavelengths are 450 nm, 525 nm and 635 nm for the nephelometer and 450, 525, 630 nm for the respective CAPS_{pmex}. The setup was described and characterised in detail in D2 in the EMPIR Black carbon project, (EMPIR-BC, 2017-2020). The main results are summarised here.

3.2 Calibration

Integrating nephelometers measure a value close to the true light scattering coefficient. However, due to the construction of the detector, only a scattering angle range of 7° to 170° is covered and the light source does not correspond to an ideal Lambertian light source as required by theory. These errors are commonly referred to as truncation errors (Anderson et al., 1996, Anderson and Ogren, 1998). For the Aurora4000 the errors were investigated in Mueller et al. (2011) and correction methods were given. The baseline value of a Nephelometer is subject to drift which must be corrected by repeated baseline measurements as a part of the overall calibration.

The CAPSpmex principle to measure the light extinction coefficient is explained in Onasch et el. (2015). This method requires the exact light path length in the measuring cell. However, the ends of the cell are highly reflective mirrors and must be protected from contamination by a purge air flow. The purge air shortens the effective light path length slightly and dilutes the sample aerosol. To correct this, a light path length factor must be introduced, which should be determined for each unit. The baseline of a CAPSpmex is subject to drift. Since the baseline drifts much more in comparison to a Nephelometer, it must be measured more frequently. Periods between 5 and 15 minutes have proven to be practical. A numerical method to improve the quality of the baseline correction was published in Pfeifer et al (2020). The absorbance measured with CAPSpmex is also sensitive to gas absorption. Regular baseline measurements correct the measured extinction for gas absorption. It should be noted that rapid changes in gas concentrations (e.g. NO2) also require more frequent baseline measurements.

The calibration of the overall setup is performed two steps:

- 1) Two-point calibration of the nephelometer with Rayleigh scattering gases, typically CO₂ and particle free air (filtered ambient air).
- 2) Cross calibration of CAPS_{pmex} and Nephelometer using non-absorbing particles. This is usually done by generating ammonium sulphate in a nebuliser. The light path length factor of CAPS_{pmex} is determined by a cross calibration between the corrected light scattering coefficient measured with the nephelometer and the measured extinction coefficient with the CAPS_{pmex}.



An uncertainty analysis was carried out which took into account all sources of uncertainty during calibration and during regular measurements. Sources of uncertainty are:

- Nephelometer noise
- Nephelometer truncation error
- Error of calibration constants of the nephelometer
- CAPS_{pmex} noise
- CAPS_{pmex} calibration error (effective light path length)
- CAPS_{pmex} baseline drift

The calculation of the particle absorption coefficient via the difference of extinction and scattering is possible with simple means. However, the description error propagation is more complicated due to the non-independent calibrations of the instruments. The full data processing chain and error propagation scheme is given in Deliverable D2 of the EMPIR black carbon project (attached as supplemental to this deliverable).

3.3 Noise

The noise characteristics of the nephelometer and the CAPS_{pmex} were determined with particle-free air. The noise, defined as the single standard deviation in an averaging interval, is plotted as a function of the length of the averaging interval (Figure 13). It is noticeable that the noise of the CAPS_{PMex} is much lower than the noise of the nephelometer especially for short averaging intervals. As the length of the averaging interval increases, the noise levels of the Aurora4000 and CAPS_{pmex} become equal.

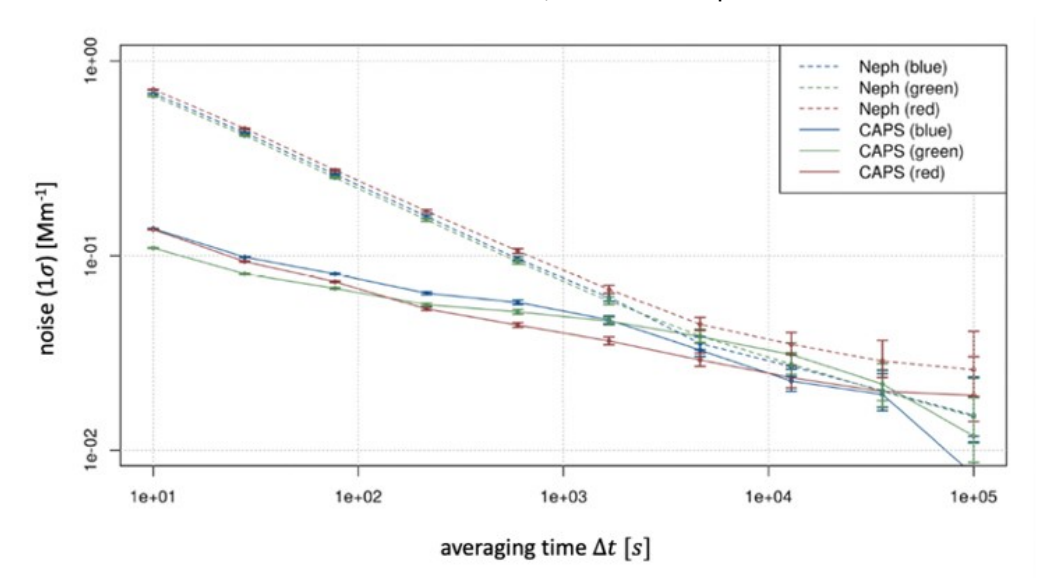


Figure 13. Noise as function of the averaging time for Nephelometer (Aurora4000) and three CAPS_{pmex} instruments (Figure taken from D2 of EMPIR Black carbon).



3.4 Repeatability of calibration factors

The repeatability of the calibrations of the entire set-up is of essential importance. For this purpose, 18 full calibrations were carried out within a period of one month. The resulting length correction factors are about 3% (635 nm and 525 nm) and 5% (450 nm) for the CAPS_{extthis} instruments. The repeatability of length correction is high with less than 2% (k=2). These errors determine the minimum EMS uncertainty with values between 3% and 5% (k=2) for cases of high concentrations and low single scattering albedos.

3.5 Uncertainty in the determination of the gas absorption coefficients

For a full evaluation of the EMS uncertainty see D2 in EMPIR black carbon. The error in light absorption coefficients varies depending on the single scattering albedo and the concentration of the aerosol under investigation. Therefore, in Figure 14, the relative error is color-coded as a function of single scattering albedo and extinction coefficient.

The errors can be relatively high for low extinction coefficients and high single scattering albedos. In order that the error does not exceed 10%, the extinction coefficient must not be less than 10 Mm⁻¹ and the single scattering albedo must not be larger than 0.95. It is easy to see that for an error of 4% extinction coefficients of about 100 Mm⁻¹ at low single scattering albedo (<0.2) are needed. For atmospheric measurements, with expected single scattering albedos between 0.7 and 0.9, extinction coefficients of about 100 Mm⁻¹ would be required to keep the error below 20%. For laboratory measurements of aerosol with high black carbon content (single scattering albedo<0.3) and concentrations with extinction coefficients of up to 500 Mm⁻¹, the error in the absorption coefficient can be less than 5%.

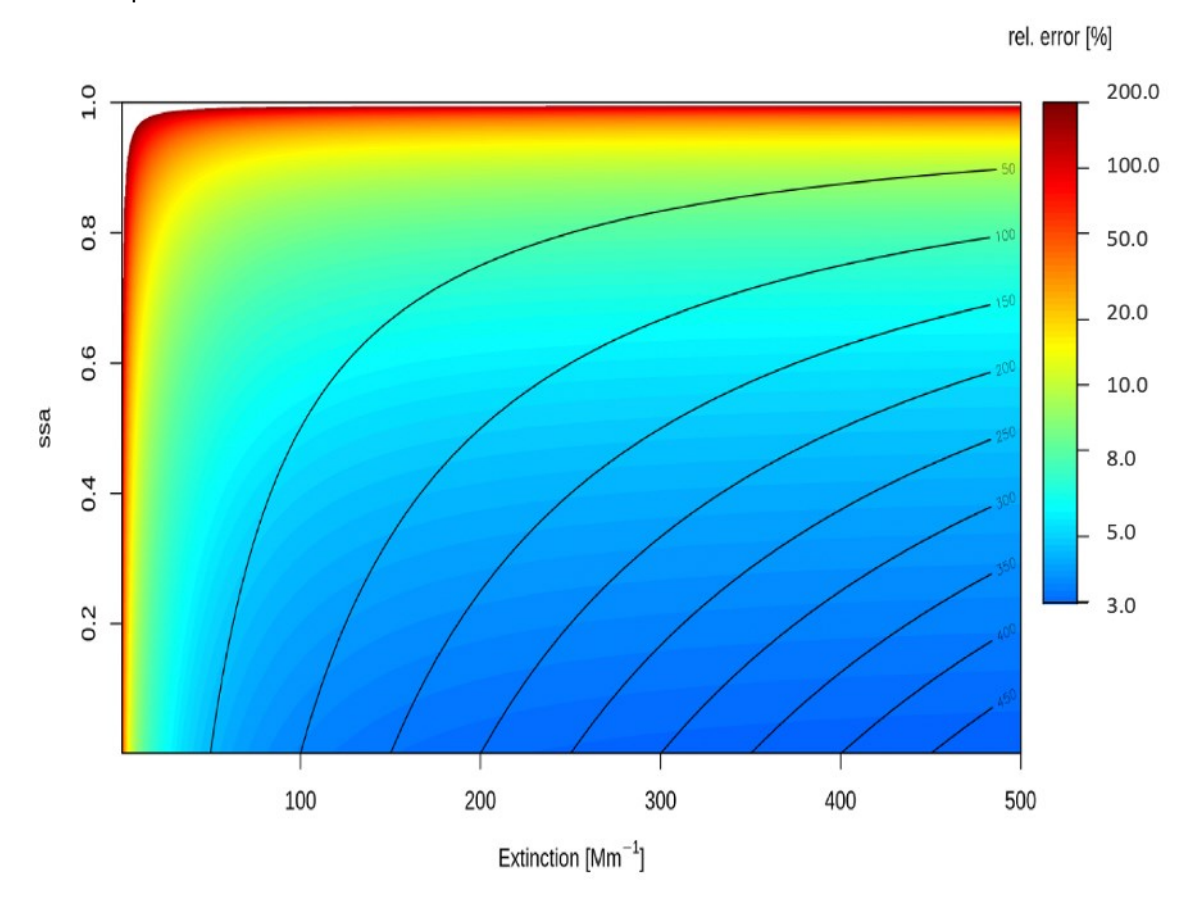


Figure 14. Relative error (k=2) of absorption coefficient at 450 nm as function of extinction coefficient and single scattering albedo for an averaging time of 60 seconds. Figure adopted from from D2 in EMPIR-BC (2017-2020)

22NRM02 STANBC



Table 5: Summary of uncertainties for Nephelometer and CAPS instruments and combined uncertainty of the EMS system. The combined uncertainty is given for conditions of high and low extinction coefficients and high and low singles scattering albedos (SSA).

		characteristic	uncertain	ty at 450	uncertain	ty at 525	uncertain	ty at 635
Source of uncertainty	contributions	time	nm		nm	_	nm	
			k=1	k=2	k=1	k=2	k=1	k=2
		60 secs		0.60/M		0.58/M		0.63/M
A: Nephelometer noise		averaging	1/Mm		0.29/Mm	-	0.32/Mm	
B: Nephelometer truncation				1 -3 %		1 -3 %		1 -3 %
		18 calibration						
C: Repeatability of CO2 calibration		s within 30 days	0.21%	0.42%	0.61%	1.22%	0.52%	1.04%
D: Systematic error of CO2 calibration (2)				3%		3%		3%
		60 secs	0.19	0.38		0.26/M		0.18/M
E: CAPS noise		averaging	/Mm	/Mm	_	-	0.09/Mm	-
F: CAPS calibration repeatability (3)			0.9 %	1.8 %	0.9 %	1.9 %	0.8 %	1.6 %
,		drift within	l	0.35/M		0.19/M		0.27/M
G: CAPS baseline stability (4)		5 minutes		m		m		m ,
H: EMS combined uncertainties, low conc (ext. coeff=50/Mm), low ssa	A, B, D, E, G	20 minutes	2.8 %	5.5%	2.1 %	4.2 %	2.1 %	4.2 %
I: EMS combined uncertainties, low conc (ext. coeff=50/Mm), high ssa (ssa=0.9)	A, B, D, E, G	20 minutes	9.5 %					
J: EMS combined uncertainties, low conc (ext. coeff=500/Mm), low ssa (ssa=0.2)	A, B, D, E, G	20 minutes	1.6 %	3.1 %	1.6 %	3.2 %	1.7 %	3.4 %
K: EMS combined uncertainties, low conc (ext. coeff=500/Mm), high ssa (ssa=0.9)	A, B, D, E, G	20 minutes	6.5 %					

⁽¹⁾ Based on scattering calculation, 1% for 'small' particles for calibration to minimize the truncation error, 3% for soot like particles

⁽²⁾ A accepted value by community based on intercompariosn of many instruments of different types

⁽³⁾ Calibration is bound to nephelometer calibration



3.6 SI-traceability

EMS is considered to be a reference method as Si-tracability for EMS can be established as follows.

The nephelometer is first calibrated with gases of known Rayleigh scattering coefficients. These are also called High and Low Span gases. Low span gas is usually particle free air. The high span gas is a gas of higher density and therefore higher Rayleigh scattering coefficient. CO₂ has become the standard against other possible gases, because the difference to the low span gas is high enough to perform a two point calibration with low uncertainty with gases of sufficient purity. The main source of error, the truncation error and the deviation of the light source from the Lambertian light source can be determined experimentally (Anderson et al. 1996, Müller et al. 2011). The correction for truncation can be calculated exactly for known gases (e.g. those used during calibration). Corrections for atmospheric aerosols with partly unknown properties can be corrected with an estimable accuracy.

The CAPS_{pmex} must be calibrated to determine the effective light path length. This is done with known non-absorbing aerosols. For this purpose, particles with a known low imaginary part of the refractive index can be used, so that the value of the light scattering is sufficiently close to the value of the light extinction. Ammonium sulfate or PSL particles are most commonly used.

Care must be taken that the aerosol transport losses to the CAPS_{pmex} and nephelometer measuring cells are equal to avoid a bias of the calibration. Therefore, it is practical to use sub-micrometer particles. The light extinction coefficient is calibration free according to the theory (Onasch et al., 2015), so that only the actual dilution factor or the effective path length is determined.

In summary, the SI traceability is established by using a high span gas with a known Rayleigh scattering coefficient, and a non-absorbing aerosol, which can be easily generated from pure inorganic salts.



4 References

Anderson, T. L. and J. A. Ogren (1998). "Determining aerosol radiative properties using the TSI 3563 integrating nephelometer." Aerosol Science and Technology 29(1): 57-69.

Anderson, T. L., et al. (1996). "Performance characteristics of a high-sensitivity, three-wavelength, total scatter/backscatter nephelometer." Journal of Atmospheric and Oceanic Technology 13(5): 967-986.

Arnott, W. P., Moosmüller, H., and Walker, J. W.: Nitrogen dioxide and kerosene-flame soot calibration of photoacoustic instruments for measurements of light absorption by aerosols, Rev. Sci. Instr., 71, 4545–4552, https://doi.org/10.1063/1.1322585, 2000.

Bluvshtein, N., Flores, J. M., He, Q., Segre, E., Segev, L., Hong, N., Donohue, A., Hilfiker, J. N., and Rudich, Y.: Calibration of a multi-pass photoacoustic spectrometer cell using light-absorbing aerosols, Atmos. Meas. Tech., 10, 1203–1213, https://doi.org/10.5194/amt-10-1203-2017, 2017.

Bogumil K,Orphal J, Homann T, Voigt S, Spietz S, Fleischmann O.C, Vogel A, Hartmann M, Bovensmann H, Frerick and Burrows J.P. 2003. "Measurements of molecular absorption spectra with the SCIAMACHY Pre-Flight Model: instrument characterization and reference data for atmospheric remote-sensing in the 230 - 2380 nm region". Journal of Photochemistry and Photobiology A: Chemistry, 157, 167-184.

Dickau, M., J. Johnson, T., Thomson, K., Smallwood, G., & S. Olfert, J. (2015). Demonstration of the CPMA-Electrometer System for Calibrating Black Carbon Particulate Mass Instruments. Aerosol Science and Technology, 49(3), 152–158. https://doi.org/10.1080/02786826.2015.1010033

Drinovec, L., Jagodič, U., Pirker, L., Škarabot, M., Kurtjak, M., Vidović, K., Ferrero, L., Visser, B., Röhrbein, J., Weingartner, E., Kalbermatter, D. M., Vasilatou, K., Bühlmann, T., Pascale, C., Müller, T., Wiedensohler, A., and Močnik, G.: A dual-wavelength photothermal aerosol absorption monitor: design, calibration and performance, Atmos. Meas. Tech., 15, 3805–3825, https://doi.org/10.5194/amt-15-3805-2022, 2022.

Elinor T. Vokes, Ernie R. Lewis, Andrew L. Johnson & Michael I. Cotterell. Densities of internally mixed organic-inorganic particles from mobility diameter measurements of aerodynamically classified aerosols, Aerosol Science and Technology, 56:8, 688-710, DOI: 10.1080/02786826.2022.2062293, 2022.

EMPIR-BC (2017-2020): 16ENV02 Black Carbon project of the European Union through the European Metrology Programme for Innovation and Research.

Flores, E., Viallon, J., Idrees, F., Moussay, P., Wielgosz, R., Shinji, U. I., Cieciora, D., Rolle, F., Sega, M., Sang-Hyub, O., Macé, T., Sutour, C., Pascale, C., Zhang, T., Wang, D., Guo, H., Han, Q., Smeulders, D., Jozela, M., Ntsasa, N. G., Tshilongo, J., Mphamo, T., Van Aswegen, S., Worton, D., Brewer, P., Valkova, M., Tarhan, T., Efremova, O., Konopelko, L., de Krom, I., Persijn, S., and van der Veen, A.: Final report on international comparison CCQM-K74: Nitrogen dioxide, 10µmol/mol, Metrologia, 58, 08018, https://doi.org/10.1088/0026-1394/58/1A/08018, 2021.

Haerri, H.-P., Macé, T., Waldén, J., Pascale, C., Niederhauser, B., Wirtz, K., Stovcik, V., Sutour, C., Couette, J., and Waldén, T.: Dilution and permeation standards for the generation of NO, NO2 and SO2 calibration gas mixtures, Meas. Sci. Technol., 28, 035801, https://doi.org/10.1088/1361-6501/aa543d, 2017.

Keller-Rudek, H., Moortgat, G. K., Sander, R., and Sörensen, R.: The MPI-Mainz UV/VIS spectral atlas of gaseous molecules of atmospheric interest, Earth Syst. Sci. Data, 5, 365–373, (2013), DOI: 10.5194/essd-5-365-2013

Mätzler, C.: MATLAB Functions for Mie Scattering and Absorption, Institute of Applied Physics, University of Bern, IAP Research Report No. 2002-08, https://omlc.org/software/mie/maetzlermie/Maetzler2002.pdf (last access: 22 June 2022), 2002.

Mie, Gustav. "Beiträge zur Optik trüber Medien, speziell kolloidaler Metallösungen". Annalen der Physik. 330 (3): 377–445. Bibcode:1908AnP...330..377M. doi:10.1002/andp.19083300302, 1908.

Moteki, N., Y. Kondo, T. Nakayama, K. Kita, L. K. Sahu, T. Ishigai, T. Kinase, and Y. Matsumi. 2010. Radiative transfer modeling of filter-based measurements of light absorption by particles: Importance of particle size dependent penetration depth. J. Aerosol Sci. 41(4):401–412. doi:10.1016/j.jaerosci.2010.02.002.

22NRM02 STANBC



Müller, T., et al. (2011). "Design and performance of a three-wavelength LED-based total scatter and backscatter integrating nephelometer." Atmospheric Measurement Techniques 4: 1291-1303.

Onasch, T. B., et al. (2015). "Single Scattering Albedo Monitor for Airborne Particulates." Aerosol Science and Technology 49(4): 267-279.

Peter F. DeCarlo, Jay G. Slowik, Douglas R. Worsnop, Paul Davidovits & Jose L. Jimenez (2004) Particle Morphology and Density Characterization by Combined Mobility and Aerodynamic Diameter Measurements. Part 1: Theory, Aerosol Science and Technology, 38:12, 1185-1205, DOI: 10.1080/027868290903907

Pfeifer, S., et al. (2020). "The influence of the baseline drift on the resulting extinction values of a cavity attenuated phase shift-based extinction monitor (CAPS PMex)." Atmospheric Measurement Techniques 13: 2161–2167.

Prahl S.; Mie Scattering Calculator. Retrieved March 31, 2011, from Mie Scattering Calculator: http://omlc.ogi.edu/calc/mie calc.html (last access: 24 May 2024), 2007.

Schnaiter, F. M., Linke, C., Asmi, E., Servomaa, H., Hyvärinen, A.-P., Ohata, S., Kondo, Y., and Järvinen, E.: The four-wavelength Photoacoustic Aerosol Absorption Spectrometer (PAAS-4λ), Atmos. Meas. Tech., 16, 2753–2769, https://doi.org/10.5194/amt-16-2753-2023, 2023.

Vandaele, A. C., Hermans, C., Fally, S., Carleer, M., Colin, R., Merienne, M. F., Jenouvrier, A., and Coquart, B.: High-resolution Fourier transform measurement of the NO2 visible and nearinfrared absorption cross sections: Temperature and pressure effects, J. Geophys. Res.-Atmos., 107, ACH 3-1–ACH 3-12, https://doi.org/10.1029/2001jd000971, 2002.

Wiedensohler, A., Wiesner, A., Weinhold, K., Birmili, W., Hermann, M., Merkel, M., ... Nowak, A. (2017). Mobility particle size spectrometers: Calibration procedures and measurement uncertainties. Aerosol Science and Technology, 52(2), 146–164. https://doi.org/10.1080/02786826.2017.1387229

Yus-Díez, J., Drinovec, L., Alados-Arboledas, L., Titos, G., Bazo, E., Casans, A., Patrón, D., Querol, X., Gonzalez-Romero, A., Perez García-Pando, C., and Močnik, G.: Characterization of filter photometer artefacts in soot and dust measurements – laboratory and ambient experiments using a traceably-calibrated aerosol absorption reference, EGUsphere [preprint], https://doi.org/10.5194/egusphere-2024-3995, 2025.

22NRM02 STANBC



5 Supplemental material

16ENV02 Black Carbon Metrology for light absorption by atmospheric aerosols - Deliverable D2





16ENV02 Black Carbon Metrology for light absorption by atmospheric aerosols - Deliverable D2

A paper describing the comparability of primary methods for aerosol optical absorption and the state-of-the-art for traceability of this metric to SI.

Coordinator: Paul Quincey, NPL

Due Date: December 2020

Submission Date: January 2021

Table of Contents

1.	Intro	duction	3
2.	Curr	ent state of the art	3
3.	Mea	surement techniques	5
	3.1.	Extinction minus scattering: Combination of Nephelometer and CAPS _{pmex}	5
	3.2.	Extinction minus scattering: Single device (CAPS _{pmssa})	11
	3.3.	Photoacoustic (PAX)	14
	3.4.	Photothermal interferometry	14
4.	Sup	porting measurements	16
5.	Sum	mary of results	21
6.	Refe	erences	26

1. Introduction

The measurement of particles in air characterized as black carbon is important both for its role in climate change and as a measure of combustion products associated with health effects. Measurements are made very widely, and compact, precise, real-time, relatively inexpensive instruments are available. Although it is conceptually a simple measure of the light absorbing properties of airborne particles, the metric does not currently have SI traceability, with consequences for the comparability and interpretation of data.

One objective of the project is to establish SI traceability for black carbon measurements. Specifically, this means to develop a traceable, primary method for determining aerosol absorption coefficients, using particulate black carbon (BC), at specific wavelengths. The method should have defined uncertainties and be quantified down to its lowest limit.

Instruments for measuring light absorption have long been the focus of research (e.g. Moosmüller et al., 2009). In this project, four types of instruments for measuring the light absorption of aerosol particles were examined in more detail for their suitability to serve as reference instruments and their traceability to SI units.

Current state of the art

Extinction Minus Scattering (EMS) techniques

The measurement of the light absorption coefficient by the difference of extinction and scattering has been used a few times in the past for laboratory measurements. The idea is that the measurement of light extinction is a fundamental optical measurement and determination of the light scattering coefficients and their uncertainties were known within certain limits. The drawback was the sensitivity of the absorbance measurements which initially limited this technique to laboratory measurements. The measurement of the light absorption coefficient by the difference of extinction and scattering has been used a few times in the past for laboratory measurements (Bond et al., 1999; Sheridan et al., 2005; Schnaiter et al., 2005). A new development of a sensitive aerosol extinction cell (CAPS_{pmex}, Aerodyne Research Inc., USA) gave this technique a boost as measurements in ambient air were now possible under certain conditions. In the earlier studies, emphasis was already put on high quality and attempts were made to prove this through comparative measurements with other types of units, so that a consistent data set could be produced. However, no traceability to SI units was established.

Photoacoustics

In photoacoustics, there have been various developments in recent years that have led to multiwavelength devices, including devices with several wavelengths integrated into one measuring cell. Also, scattering measurements have been integrated together with photoacoustic cells. In the following, some of the main development steps are presented. The first portable photoacoustic instruments for measuring the aerosol light absorption coefficient with detection limits less than 1 Mm⁻¹ were developed in the 1990s at wavelengths of 532 and 685 nm (Arnott et al., 1999) and near-IR (802 nm) (Petzold et al., 1995). Lack et al. (2006) demonstrated enhanced sensitivity by employing a multi-pass laser (532 nm) alignment with a limit of detection of 0.08 Mm⁻¹. Lewis et al. (2008) integrated two lasers (405 and 870 nm) in a single photoacoustic cell. That instrument was later extended into a three-wavelength (405, 532, 781 nm) version commercialized as the PASS-3 (Droplet Measurement Technologies; Boulder, CO). A combined photoacoustic extinctiometer with integrated inverse nephelometer for measuring the light scattering coefficient and photoacoustic cell for measuring the absorption coefficient was developed by DMT (Droplet Measurement Technologies; Boulder, CO). This instrument is available at wavelengths of 405, 530 and 870 nm. On instrument with a special wavelength of 375 nm was intensively characterized by Nakayama et al. (2015).

Photothermal Interferometry

Photothermal interferometry (PTI) is an in-situ direct absorption measurement technique first applied to gas absorption but also applied to aerosol measurements (Sedlacek et al., 2007; Lee and Mossmüller, 2020). In PTI, the light absorption of a sample is measured by probing changes in the refractive index of the sample due to light absorption using interferometry. Previous realisations of PTI require two lasers, one of high power that is modulated and absorbed by the sample (pump), and a second CW interferometry laser (probe). The detection limit of PTI has been found for aerosol measurements larger than 0.2 Mm⁻¹ (Sedlacek et al., 2007). The difficulties associated in achieving low detection limits in the conventional PTI setups are related to the sensitivity of interferometric measurements to external noise sources, the difficulty of optimally aligning and maintaining the alignment of the pump and probe beams, and measurement artefacts due to cross-sensitivity to other absorbing species, such as NO₂, volatile organic compounds (VOC) and O₃.

3. Measurement techniques

3.1. Extinction minus scattering: Combination of CAPS_{pmex} and Nephelometer

Measurement setup

The setup described here consists of a three-wavelength nephelometer Aurora4000 (Ecotech Pty LTD , Australia) and three CAPS $_{pmex}$ (Aerodyne Research, Inc., USA) devices. The wavelengths are 450 nm, 525 nm and 635 nm for the nephelometer and 450, 525, 630 nm for the respective CAPS $_{pmex}$. Due to the design with a total of four separate cells for measuring scattering and extinction, care was taken to minimise particle transport losses to all instruments and, very important, to ensure that the losses are similar. Since different losses can occur especially for coarse mode particles, it is recommended to use a pre-separator (PM $_1$).

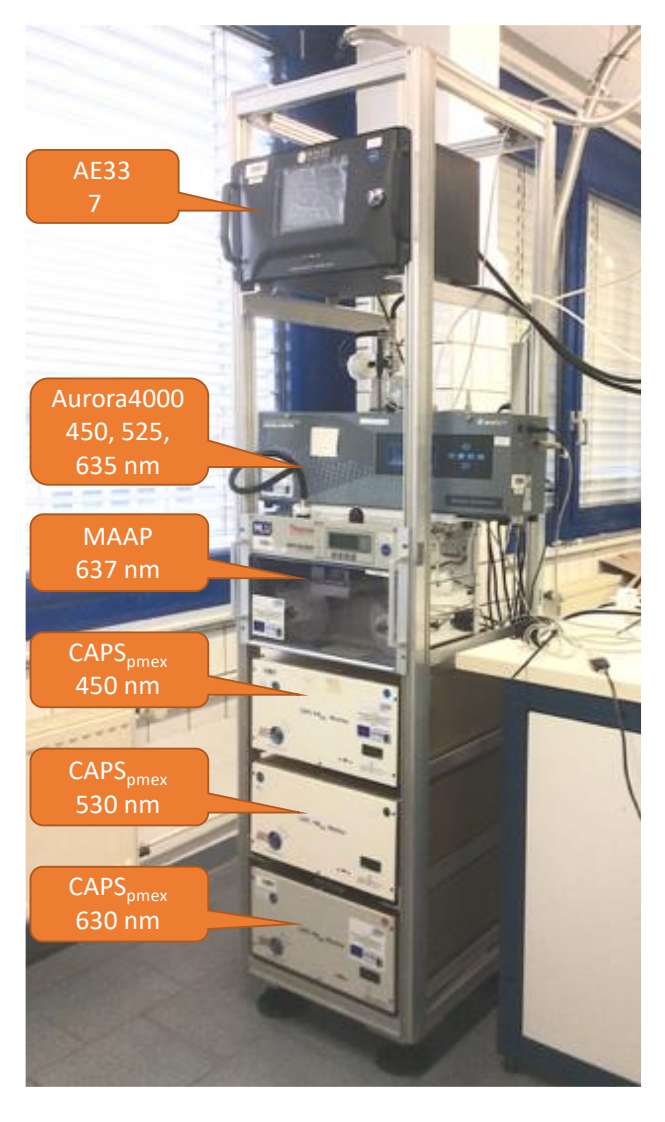


Figure 3.1.1: Photography of the setup as it was used for the TROPOS generator experiment 2019. In addition to the three CAPS_{pmex} and the Aurora4000, a MAAP and an AE33 aethalometer are also integrated.

Instrument corrections and calibration

To determine the light absorption coefficient, the instruments must be calibrated and the values corrected. First, the necessary corrections are introduced, as these are also essential for calibration.

Integrating nephelometers measure a value close to the true light scattering coefficient. However, due to the construction of the detector, only a scattering angle range of 7° to 170° is covered and the light source does not correspond to an ideal Lambertian light source as required by theory. These errors are commonly referred to as truncation errors (Anderson et al., 1996, Anderson and Ogren, 1998). For the Aurora4000 the errors were investigated in Mueller et al. (2011) and correction methods were given. It must be emphasized, that the truncation error increases with increasing particle size and its correction also becomes more uncertain. The baseline value of a Nephelometer is subject to drift which must be corrected by repeated baseline measurements. It has been found that under optimal conditions, i.e. stable temperatures and low aerosol humidity, it is sufficient to measure the baseline once a day.

The CAPS_{pmex} principle to measure the light extinction coefficient is explained in Onasch et el. (2015). This method requires the exact light path length in the measuring cell. However, the ends of the cell are highly reflective mirrors and must be protected from contamination by a purge air flow. The purge air shortens the effective light path length slightly and dilutes the sample aerosol. To correct this, a light pathlength factor (see also chapter 3.2) must be introduced, which should be determined for each unit. The baseline of a CAPS_{pmex} is subject to drift. Since the baseline drifts much more in comparison to a Nephelometer, it must be measured more frequently. Periods between 5 and 15 minutes have proven to be practical. Since a baseline measurement takes up to 2 minutes, the loss of data seems to be very high. However, for the calculation of the absorption from the difference of extinction and scattering, the data quality is very important and the loss of data during the baseline periods has to be accepted. Furthermore, a numerical method to improve the quality of the baseline correction was published in Pfeifer et al (2020). The absorbance measured with CAPS_{pmex} is also sensitive to gas absorption. Regular baseline measurements correct the measured extinction for gas absorption. It should be noted that rapid changes in gas concentrations (e.g. NO2) also require more frequent baseline measurements.

The calibration of the overall setup is performed by the following two steps:

- 1) Two point calibration of the nephelometer with Rayleigh scattering gases, typically CO₂ and particle free air.
- 2) Cross calibration of CAPS_{pmex} and Nephelometer using non-absorbing particles. This is usually done by generating ammonium sulphate in a nebuliser. The light path length factor of CAPS_{pmex} is determined by a cross calibration between the corrected light scattering coefficient measured with the nephelometer and the measured extinction coefficient with the CAPS_{pmex}.

An error analysis was carried out which took into account all sources of errors during calibration and during regular measurements. Sources of errors are:

- Nephelometer noise
- Nephelometer truncation error
- Error of calibration constants of the nephelometer
- CAPS_{pmex} noise
- CAPS_{pmex} calibration error (effective light path length)
- CAPS_{pmex} baseline drift

The calculation of the particle absorption coefficient via the difference of extinction and scattering is possible with simple means. However, the description error propagation is more complicated due to the non-independent calibrations of the instruments. The full data processing chain and error propagation scheme is shown in Figure 3.1.2.

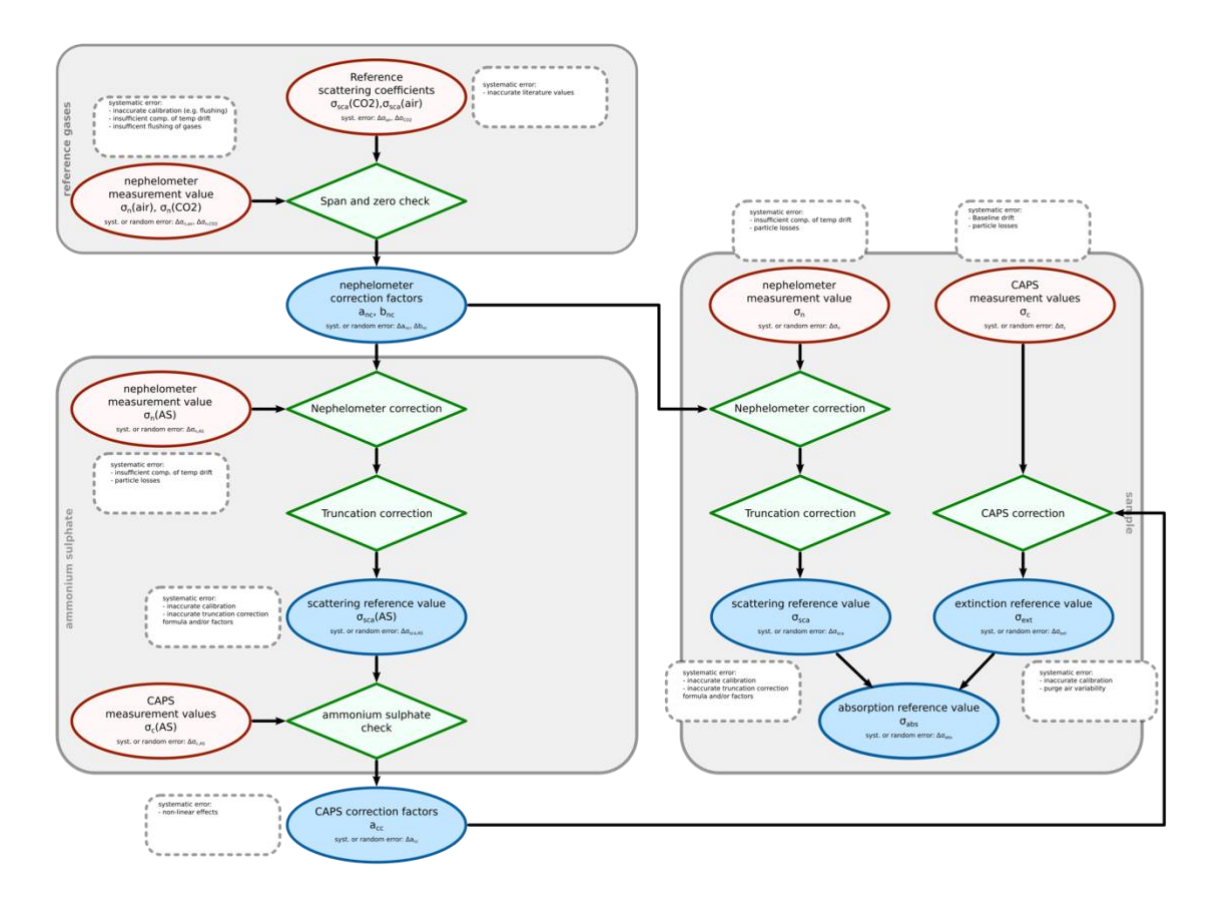


Figure 3.1.2: Calibration chain and error propagation of a setup for measuring the particle absorption coefficient by the difference of particle extinction and scattering coefficients.

Instrumental noise

The noise characteristics of the nephelometer and the CAPS_{pmex} were determined by a ten-day measurement with particle-free air. The noise, defined as the single standard deviation in an averaging interval, is plotted as a function of the length of the averaging interval (Figure 3.1.3). It is noticeable that the noise of the CAPS_{PMex} is much lower than the noise of the nephelometers especially for short averaging intervals. As the length of the averaging interval increases, the noise levels of the Aurora4000 and CAPS_{pmex} become equal. It is suspected that a non-gaussian source of error (e.g. baseline drift) is causing the weaker decrease of noise in the CAPS_{pmex}.

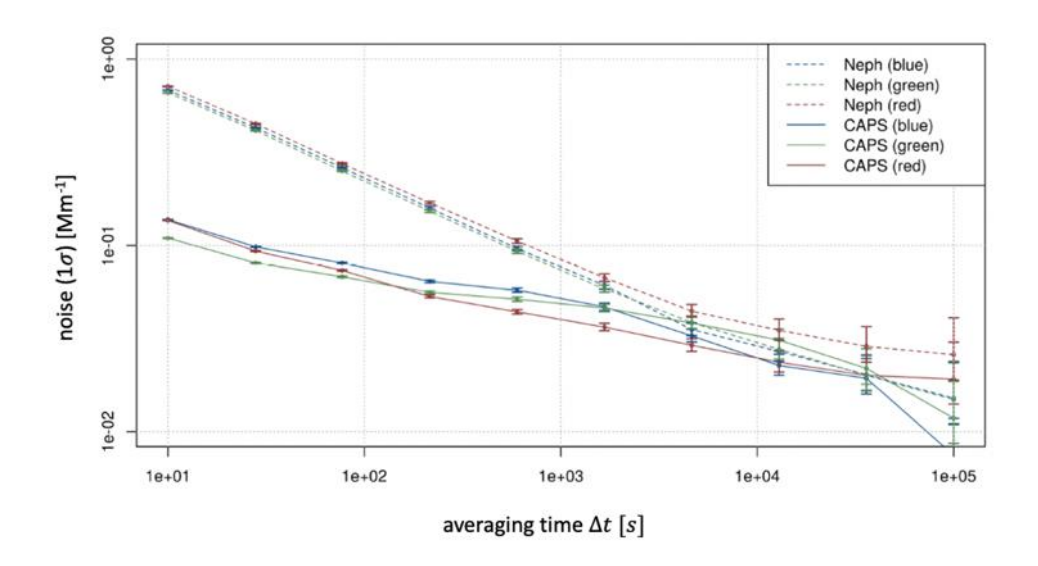


Figure 3.1.3: Noise as function of the averaging time for Nephelometer (Aurora4000) and three CAPS_{DMEX} instruments.

Long term stability of the path length calibration factor of CAPS_{pmex}

The repeatability of the calibrations of the entire set-up is of essential importance. For this purpose, 18 full calibrations were carried out for a period of about one month. The resulting light path length correction factors are shown in Figure 3.1.4. These factors also include the uncertainties of the nephelometer calibrations due to the cross calibration, which are between 2 and 3%. Two instruments (630 nm and 532 nm) agree well, while the third instruments (450 nm) is about 5% higher. However, this graph reflects the repeatability of the overall EMS calibration, which is about $\pm 2\%$.

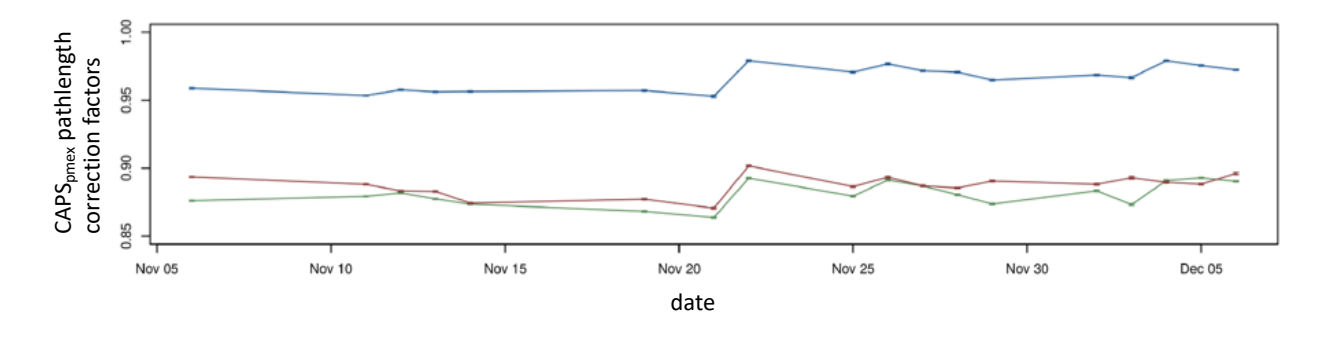


Figure 3.1.4: Series of repeated calibrations of the light pathlength factor of three CAPSpmex.

For these measurements, the setup was changed as little as possible over the entire period and not moved. Transporting the setup would require a recalibration, as nephelometers in particular are sensitive to transportation if not handled carefully (pers. communication, Sascha Pfeifer 2020).

Interdependences of calibration constant

In the following, the interdependencies of the calibration constants are discussed. The nephelometer provides two calibration constants for each wavelength, one for the CO₂ calibration

(slope of two point calibration) and the other for the baseline. The CAPS_{pmex} also has two calibration constants, the effective light path length and the baseline. Since the baseline of the CAPS_{pmex} is adjusted several times within a full calibration, it is not included here as a calibration parameter.

The correlation between the remaining three calibration constants for three wavelengths each is shown in a correlation matrix (Figure 3.1.5). It is noticeable that the three baseline constants of the nephelometer correlate with each other. This may mean that either contamination of the cell has occurred or that there is an influencing factor in the electronics or opto-electronic components that affects all wavelengths equally. The CO₂ calibration factors on the other hand are less correlated. Another block with negative correlations can be seen between the nephelometer baseline and the CAPS_{pmex} path length factor. This negative correlation allows the conclusion that the current baseline values of the nephelometer calibration influence the overall system to a large part. It could not be worked out whether technical improvements or an optimized measurement strategy for performing the calibration would lead to an improvement.

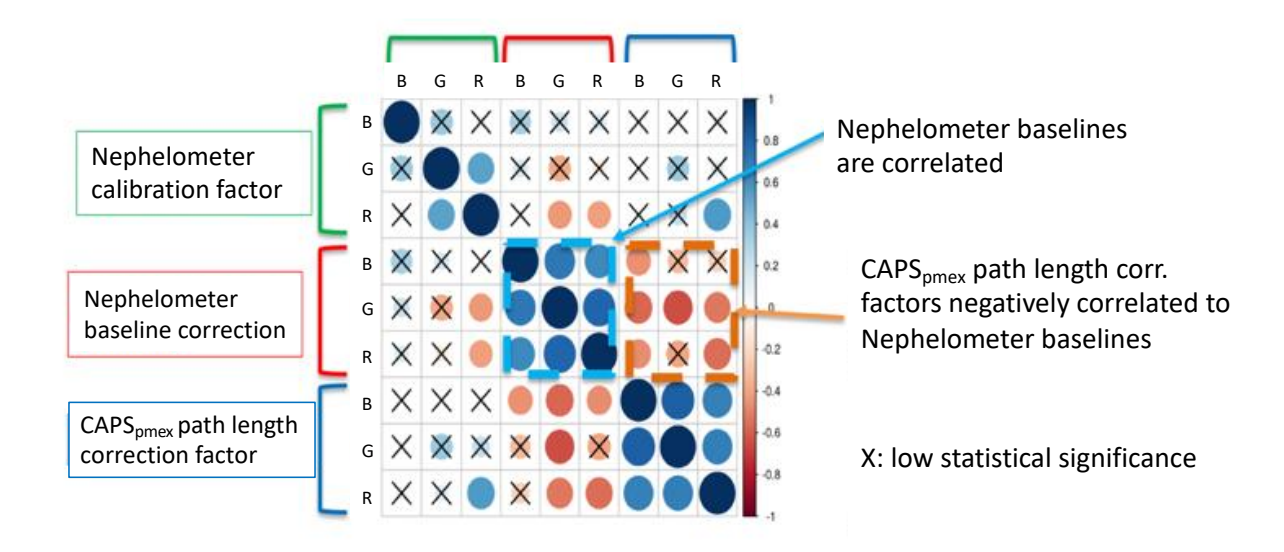


Figure 3.1.5: Correlation matrix of calibration constants, wherein *B*, *G* and *R* denote wavelengths 450 nm, 530 nm and 630 nm.

Error of absorption coefficients

The error calculation was performed according to the scheme shown in Figure 3.1.2 and the respective determined uncertainties were applied. The error varies depending on the single scattering albedo or the concentration of the aerosol under investigation. Therefore, in Figure 3.1.6, the relative error is color coded as a function of single scattering albedo and extinction coefficient.

The errors can be very high for low extinction coefficients and high single scattering albedos. In order that the error does not exceed 10%, the extinction coefficient must not be less than 10 Mm⁻¹ and the single scattering albedo must not be larger than 0.95. It is easy to see that for an error of 4% extinction coefficients of about 100 Mm⁻¹ at low single scattering albedo (<0.2) are needed. In the field, with expected single scattering albedos between 0.7 and 0.9, extinction coefficients of about 100 Mm⁻¹ would be required to keep the error below 20%.

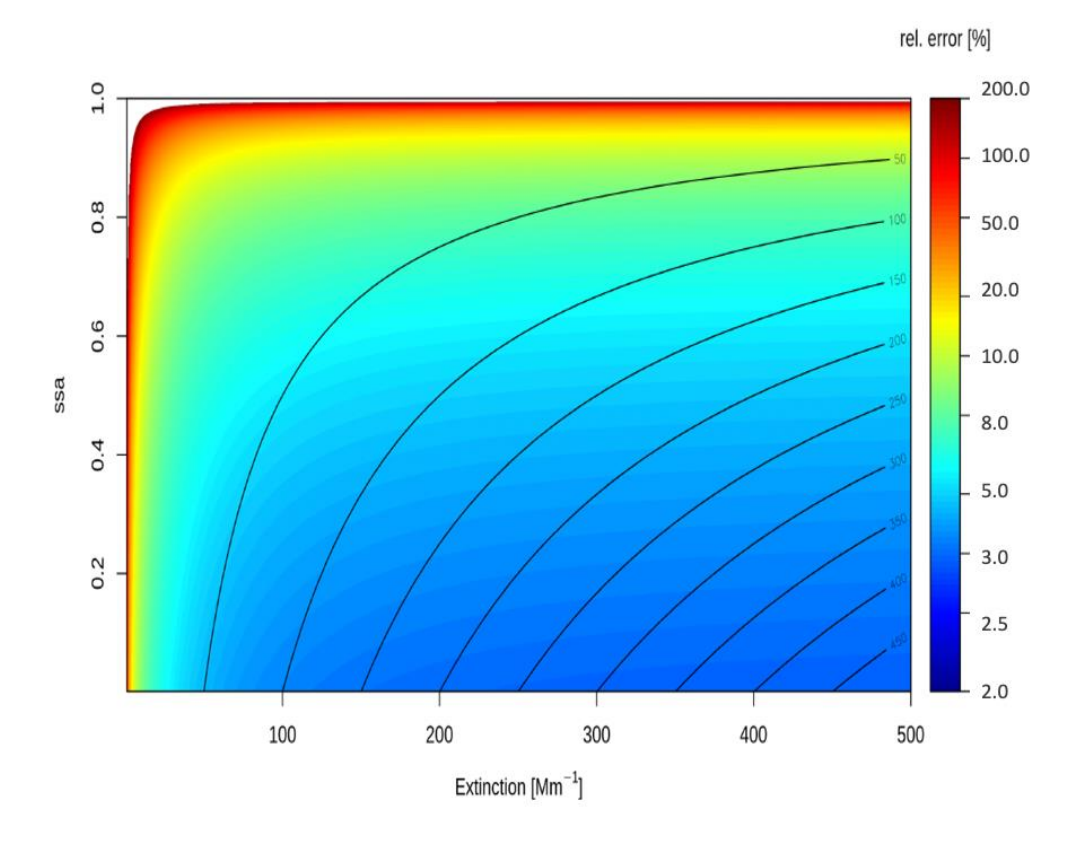


Figure 3.1.6: Calculated relative error (k=2) of absorption at 450 nm as function of extinction coefficient and single scattering albedo.

SI-traceability

The nephelometer is first calibrated with gases of known Rayleigh scattering coefficients. These are also called High and Low Span gases. Low span gas is usually air (particle free). This gas can be from filtered ambient air or from a gas cylinder. This gas is also used for recurring baseline measurements, so filtered air has become the standard. The high span gas is a gas of higher density and therefore higher Rayleigh scattering coefficient. CO₂ has become the standard against other possible gases, because the difference to the low span gas is high enough to perform a two point calibration with low uncertainty and because it is easy to handle and also available in sufficient purity. The measurement of the optical properties, the Rayleigh scattering coefficients, is carried out with an optical system whose geometry can be reproduced with simple means to ensure correct operation. The main source of error, the truncation error and the deviation of the light source from the Lambertian light source can be determined experimentally (Anderson et al. 1996, Müller et al. 2011). The correction for truncation can be calculated exactly for known materials (e.g. those used during calibration). Corrections for atmospheric aerosols with partly unknown properties can be corrected with an estimable accuracy.

The CAPS_{pmex} must be calibrated to determine the effective light path length. This is done with known non-absorbing aerosols. For this purpose, particles with a known low imaginary part of the refractive index can be used, so that the value of the light scattering is sufficiently close to the value of the light extinction. Ammonium sulfate or PSL particles are most commonly used.

Care must be taken that the aerosol transport losses to the CAPS_{pmex} and nephelometer measuring cells are equal to avoid a bias of the calibration. Therefore, it is practical to use submicrometer particles. The light extinction coefficient is calibration free according to the theory

(Onasch et al., 2015), so that only the actual dilution factor or the effective path length is determined. However, it has been shown that at high light extinctions (>1000 Mm-1) a non-linearity can occur. If the non-linear range is not reached, the instrument can be used without any restriction.

3.2. Extinction minus scattering: Single device (CAPS_{pmssa})

The CAPS_{pmssa}, manufactured by Aerodyne Research Inc. (USA) and described in Onasch et al. (2015), combines the extinction cell of the CAPS_{pmex} with an integrating sphere nephelometer built around it (Figure 3.2.1). A key advantage of this instrument is that both extinction and scattering measurements probe the identical aerosol due to the common detection volume. A challenge is truncation of scattered light due to the openings in the sphere and light reflections at the glass tube guiding the aerosol, which results in a reduction of light collection efficiency.

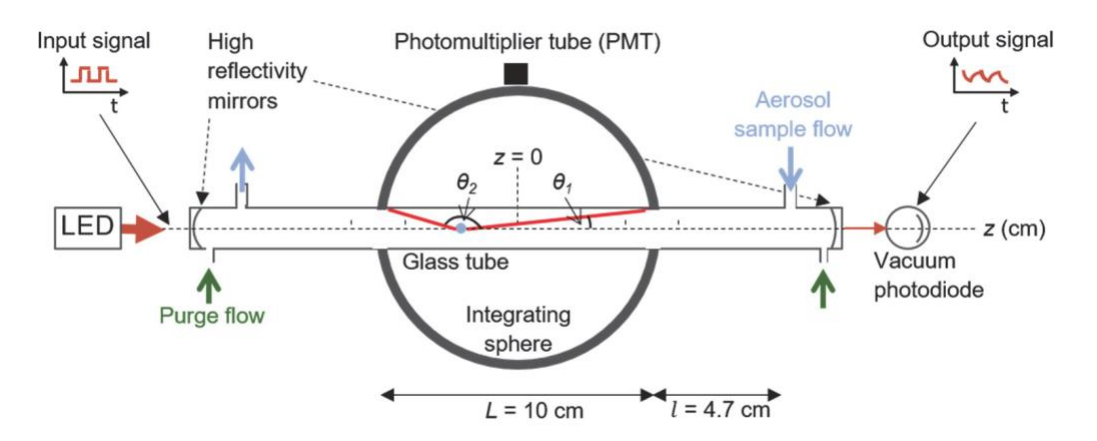


Figure 3.2.1: Schematic representation of the combined extinction and scattering measurements in a cell. The angles θ_1 and θ_2 indicate the truncation angles of light scattered by particles at one point in the scattering cell (Figure taken from Modini et al. 2021).

The original technical paper did not consider the contribution of reflections at the glass tube to truncation. An extensive experimental characterization of the truncation function and general performance of the CAPS_{pmssa} was performed as part of the EMPIR Black Carbon project (Modini et al., 2021). This study confirmed the truncation enhancement by reflections. Observed truncation agrees within uncertainty with theoretically expected curves, where the remaining uncertainty is dominated by unknown laser path length outside the integrating sphere from which light can be scattered into the sphere. The uncertainty associated with truncation correction is estimated to be ~4% and 9% for fine and coarse mode dominated aerosol, respectively. Therefore, it is recommended to restrict CAPS_{pmssa} based absorption coefficient measurements to submicron-sized aerosol, i.e. to remove coarse particles using an impactor.

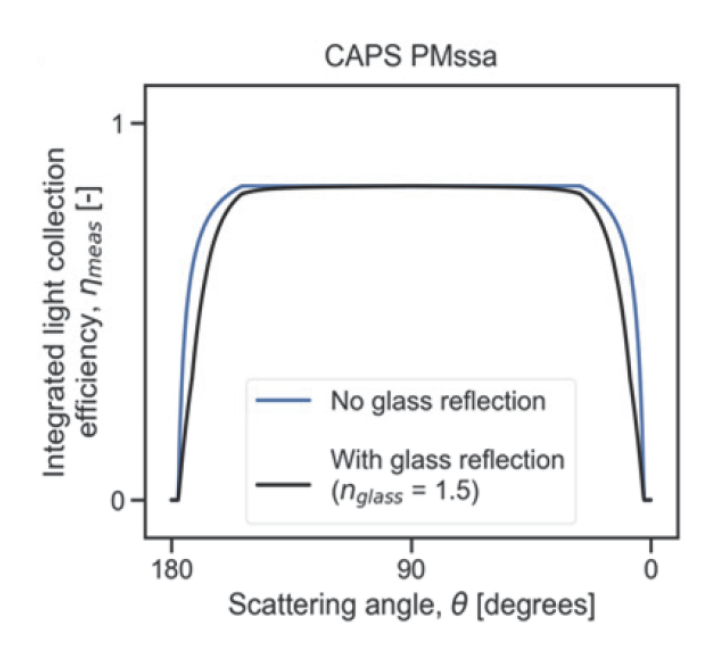


Figure 3.2.2: Illustration of the angle-dependent efficiency of light collection by truncation and passage through the glass tube (Figure taken from Modini et al., 2021).

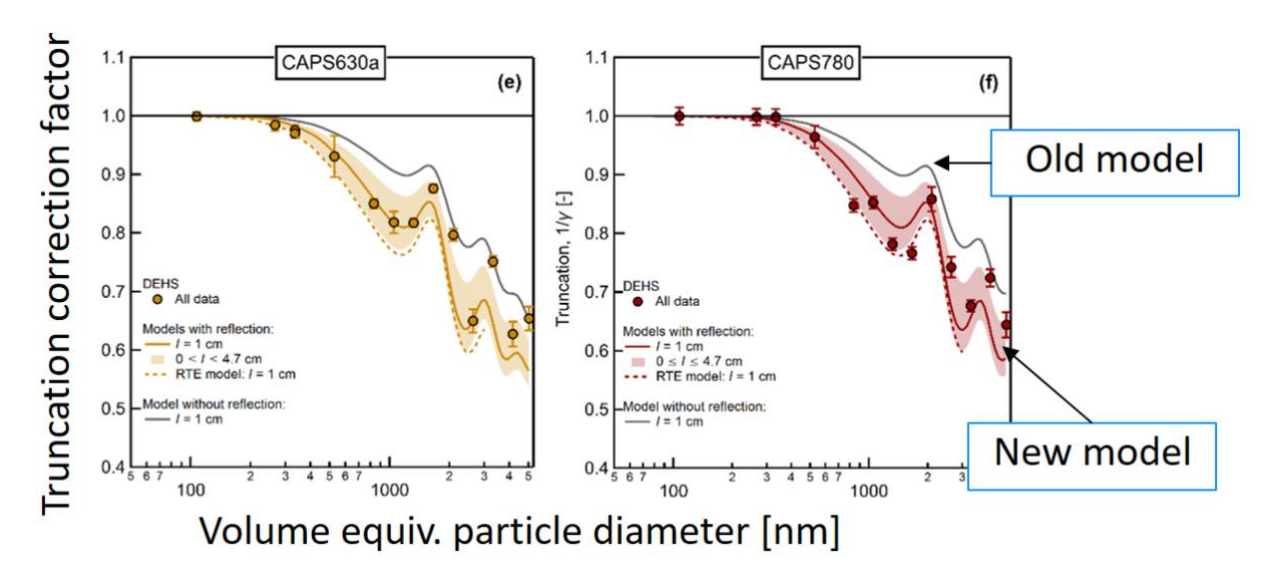


Figure 3.2.3: Truncation correction factor for two CAPS_{pmssa} at wavelength 630 and 780 nm. The new model including glass reflections agrees significantly better with measurements for fine mode particles compared to the model without reflections. (adapted from Modini et al., 2021)

The CAPS_{pmssa} is not fully traceable on its own as the effective path length relevant to the extinction measurement can vary between instruments and drift over time (Petzold et al. 2013, Pfeifer et al. 2020). Furthermore, a non-linearity was observed at high total loss (>1000 Mm⁻¹), whereas the degree of non-linearity varies between instruments. Therefore, the extinction channel needs to be referenced against a calibrated nephelometer using parallel measurements of a suitable non-absorbing aerosol. This makes it possible to determine the effective path length with 1% uncertainty (Pfeifer et al. 2020). The scattering channel of CAPS_{pmssa} is cross-calibrated against the extinction channel using sufficiently small aerosol particles with known phase function of Rayleigh scatters to minimize uncertainties. The scattering cross calibration factor can be determined with a precision of around 2% (Modini et al. in press).

The uncertainties in the measurements of the extinction and scattering coefficients were extensively studied. Both precision and drift (stability based uncertainty) were considered. The corresponding values are given in Table 1 in Modini et al. (2021). The combined uncertainties, here the relative error of the absorption coefficients, are shown in Figure 3.2.4. Note that the error depends on the averaging time, the single scattering albedo and the value of the extinction coefficient. Differences in error for the three examples shown in Figure 3.2.4 are primarily associated with differences in stability based uncertainty for different instrument units, which were identified by repeated calibrations.

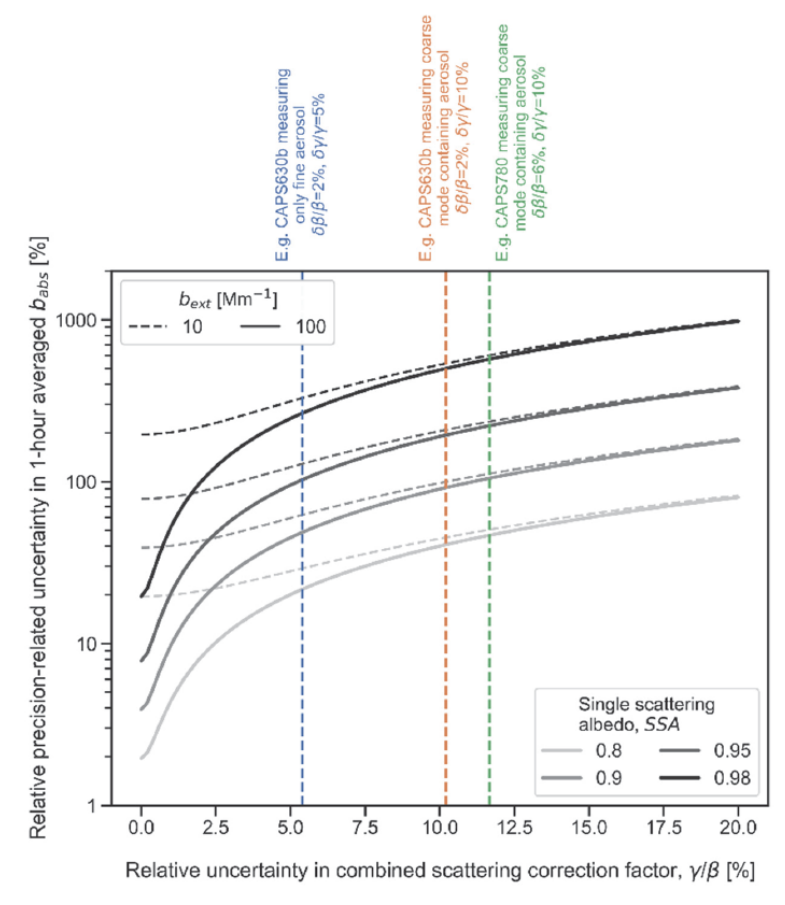


Figure 3.2.4: Calculated relative uncertainties for one-minute averages of the absorption coefficients. The abscissa shows the combined uncertainty factor of the scattering correction factors, with three values marked for special cases. For details on the uncertainty factor, we refer to Modini et al. (2021). The curves are for four singles scattering albedos, each with high (straight lines) and low (dashed lines) extinction coefficients. Figure adopted from Modini et al., (2021).

As pointed out in the literature, the purge flows that protect the high reflectivity mirrors shorten the effective optical path length of the cavity and slightly dilute the instrument sample flow. Therefore, a correction factor must be applied to in order to account for these changes (Massoli et al., 2010; Onasch et al., 2015; Petzold et al., 2013). The correction factor was shown to vary less than 3% over a period of about one year for CAPS_{pmex} (Pfeifer et al. 2020). However, this result was obtained under optimal laboratory conditions and may not be applied to equipment in the field, especially after transport. The CAPS_{pmssa} is therefore not a stand-alone SI traceable system. It can be used as a secondary reference by cross calibrating with a nephelometer. The need and frequency to perform cross calibrations will then depend on the application.

3.3. Photoacoustic (PAX)

PAX measures the particles' light absorption and scattering coefficients using a photo-acoustic cell and an inverse nephelometer. Thus, the particle extinction coefficient and the single scattering albedo can be determined directly. The light scattering is calibrated by non-absorbing particles, e.g. PSL or ammonium sulfate, in high concentrations and by a comparison with the internally measured light extinction. The calibration of the absorption coefficient is performed by comparing the photo-acoustic intensity and the light extinction with a strongly absorbing aerosol. Uncertainties due to neglecting the truncation error of the scattering channel and the single scattering albedo during the calibration of the absorption cell are not fully known. There are additional uncertainties connected to linearity, as calibration is typically carried out at relatively high concentrations, humidity and evaporation effects. Due to the calibration method and the inherent uncertainties, the device is not SI-traceable.

A comparison of the PAX with the CAPS_{pmex}-Aurora4000 was carried out in parallel to the TROPOS generator intercomparison experiment 2019. Results of this intercomparison are shown in Chapter 4. The noise (1σ) for a 10 second averaging time of the absorption and scattering coefficients was determined to be 0.57 Mm⁻¹ and 0.52 Mm⁻¹, respectively.

3.4. Photothermal interferometry

Method description

The measurement principle of the new photothermal interferometry (PTI) that has been developed within this project has been described in detail in a recent publication (Visser et al, 2020) and therefore presented in a brief form here. The Authors direct the interested reader to the aforementioned publication for more details.

Photothermal interferometry measures the temperature increase caused by the absorption of light by a light absorbing substance. In the case of aerosol measurements, the temperature increase of the air is measured after light absorption by impurities in the air such as BC particles and NO₂ gas. By modulating the laser irradiation of the sample, a temperature modulation of the air occurs, the amplitude of which is directly proportional to light absorption coefficient of the aerosol. The temperature modulation causes a modulation of the local air density and thus a modulation of the refractive index of the air. This modulation of the refractive index can then be measured via interferometry.

Previous PTI designs have relied upon two lasers, one extremely stable laser for interferometry and another higher-powered laser, whose beam is amplitude modulated and absorbed by the light absorbing substances in the air. In the realization of PTI presented here (Figure 3.4.1), the two lasers have been replaced by a single highly stable and high-powered laser (532 nm wavelength), which is amplitude modulated. This development is termed modulated single-beam interferometry (MSPTI).

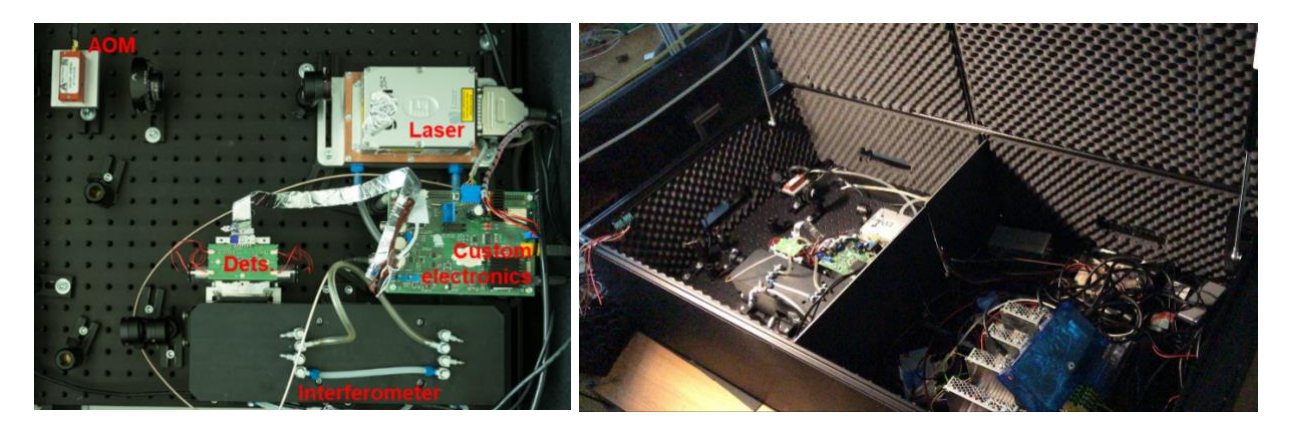


Figure 3.4.1: The newly developed MSPTI. Left: top view of the sensor unit. Right: Whole MSPTI with sensor unit and power supply and data acquisition.

Compensation of trace gases

The instrument has been designed such that measurements of BC are free of artifacts caused by absorbing gases such as NO₂. A reference chamber is filled with the filtered ambient aerosol and any light absorption in this chamber is automatically subtracted from the total aerosol light absorption. To our knowledge, this is the first time that this has been achieved in an in-situ measurement of light absorption.

The current prototype instrument has been significantly improved from the version that is presented in our recent publication (Visser et al., 2020). The interferometer is now constructed in a solid metal housing, the pressure chamber for controlling the quadrature point has been incorporated into the aerosol chamber and the quadrature point is controlled by a custom bellows. Furthermore, the commercial electronics units have been replaced by custom-built solutions. An updated schematic of the MSPTI is shown in Figure 3.4.2.

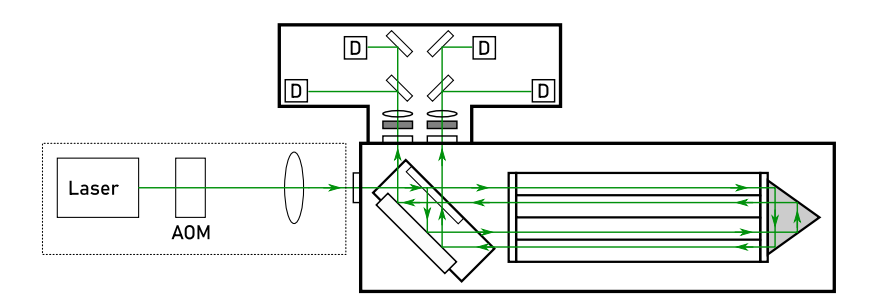


Figure 3.4.2: Schematic of the current sensor unit in the MSPTI instrument.

Calibration

The MSPTI is calibrated using NO₂ gas. By switching from measurement mode to calibration mode the measurement chamber is filled with NO₂ gas and the reference chamber is filled with filtered lab air. The measured absorption is then compared to the literature absorption cross-section of NO₂ at the laser wavelength. This means that the MSPTI can be calibrated to a traceable primary reference and used to calibrated other light absorption-based instruments. For more information see Visser et al. (2020).

Detection limit and error analysis

The current detection limit (1σ) of the MSPTI is approximately 0.4 Mm⁻¹ for NO₂ gas and an averaging time of 120 seconds (Figure 3.4.3). It is up to a factor of two higher for BC particles due to statistical noise arising from very low numbers of particles in the detection volume at such low concentrations. This statistical noise is still subject to investigation.

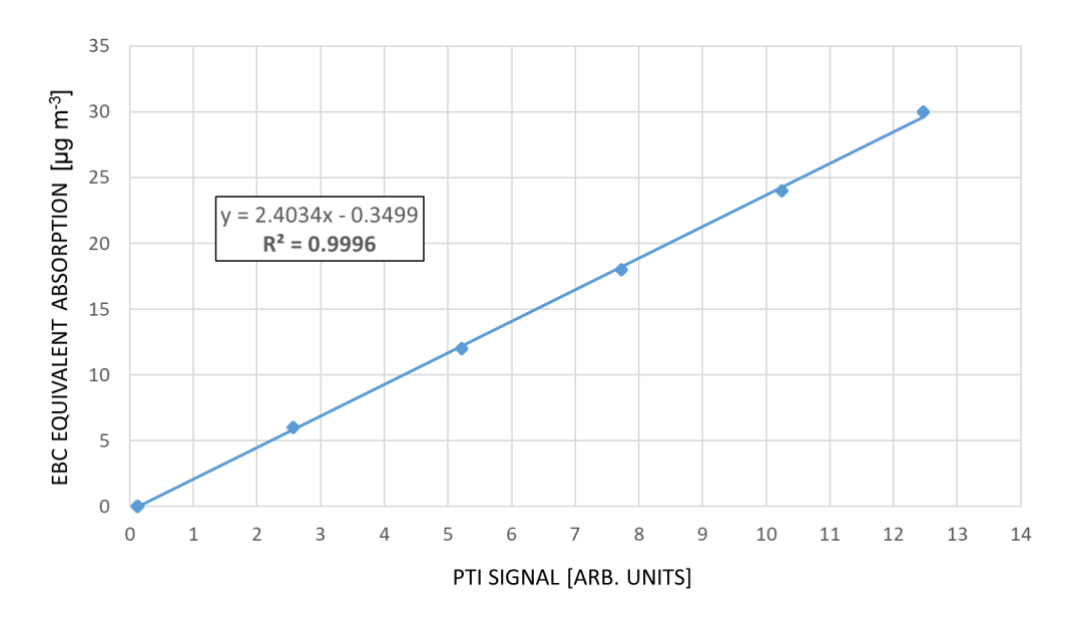


Figure 3.4.3: Concentration series showing that the current detection limit is 0.4 Mm⁻¹. This corresponds to an eBC concentration of 40 ng m⁻³ (assuming a mass absorption coefficient of 10 m²/g).

The main sources of error are related to the stability of the laser. Changes in lasing wavelength can be falsely interpreted as changes in absorption. The stability of the background measurement is also influenced by the laser stability and it is important to account for background drifts by measuring the background absorption every few minutes.

4. Supporting measurements

A laboratory experiment was conducted to compare the optical properties of different soot sources. Different instruments were also used to measure the light absorption coefficient. As this experiment was not intended as the main experiment for comparing instruments, not all instruments were available. Planned joint comparison experiments could not be carried out because of COVID-19. Therefore, we can only present data that support our results.

The generated aerosol particles were diluted with dry particle-free air and fed to a 0.5 m³ chamber at low relative humidity. The aerosol was then analysed by several online instruments including three CAPS_{pmex} (450, 530, 630 nm, Aerodyne Research, USA), one CAPS_{SSA} (670 nm, Aerodyne Research, USA), a MAAP (637 nm, Thermo Scientific, USA), an Aethalometer (7 wavelengths AE33, Magee Scientific, USA), a micro-soot sensor (MSS, AVL, Austria), a PAX (870 nm, Droplet Measurement Technologies, USA), a nephelometer (Aurora 4000, Ecotech, Australia), an SMPS (TROPOS, Germany), a TEOM (model 1405, Thermo Scientific, USA), and a Quartz Crystal Microbalance (QCM) MOUDI (Thermo Scientific, USA). Passive samplers were used to collect

samples for TEM, EC/OC analysis and Raman microspectroscopy. The setup is show in Figure 4.1 and overview of the BC sources is given in Table 4.2.

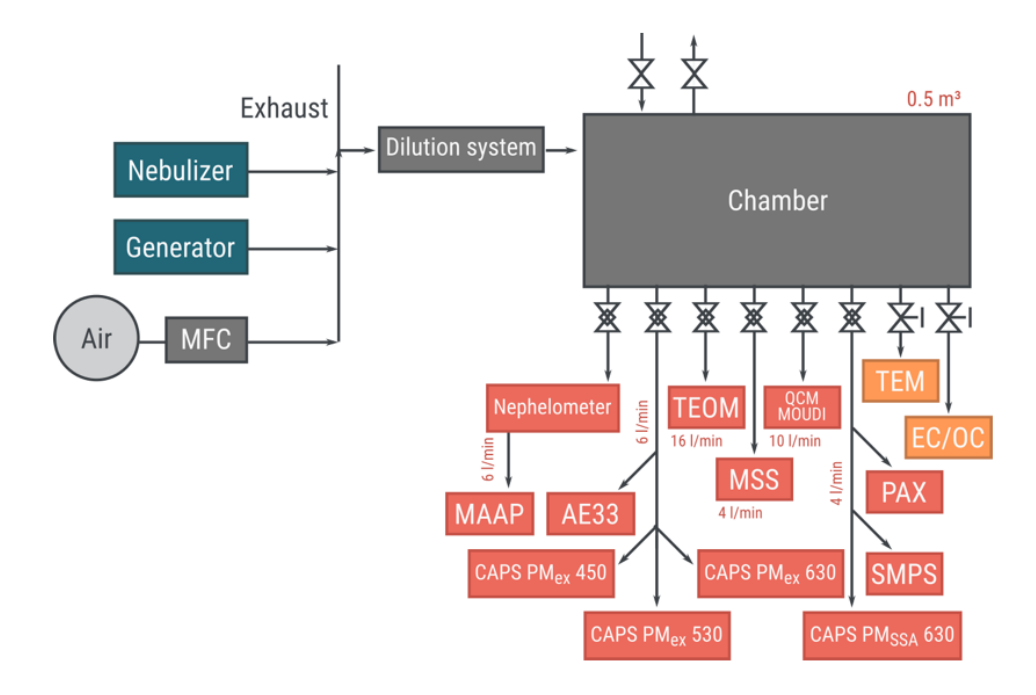


Figure 4.1: Schematic diagram of the instrumental setup for the TROPOS generator intercomparison workshop.

Table 4.1: Reference instruments

Technik	EMS	EMS	Photoacoustic extinctiometer
Instrument	CAPS _{pmex} - Aurora4000	CAPS _{pmssa}	PAX
Comment	Instruments as described in chapter three. Calibrated before experiments.	Device with wavelength 670 nm. Calibrated after BC experiments.	Instruments as described in chapter three, Calibrated before experiments.

Table 4.2: Compilation of properties of soot from all experiments done. Beside the geometric and volume mean diameter, also the single scattering albedo(ssa), absorption and scattering Ångström exponents (AAE and SAE), mass absorption cross section (MAC) and the EC/TC ratio are given. Data are taken from in deliverable D1 (Table 1 therein).

#	Generator	Geometric mean diameter (nm)	Volume Mean Diameter (nm)	SSA (-)	AAC (-)	MAC (m²/g)	EC/TC (-)
1	mini-CAST 5201BC	106±11	173±13	0.04±0.01	1.15±0.06	4.2	0.66
2	mini-CAST 5201BC	71±3	124.5	(870 nm)	4 42 : 0 05	(870 nm)	0.60
2	IIIIII-CAST SZOIBC	71±5	124±5	0.02±0.01 (870 nm)	1.12±0.05	3.74 (870 nm)	0.68
3	mini-CAST 5201BC	43±2	82±3	0.01±0.03	1.15±0.11	5.68	0.34
				(870 nm)		(870 nm)	
4	mini-CAST 5203C(PTB)	92±2	156±2	0.08±0.09	1.27±1.41		0.44
				(870 nm)	1		
5	mini-CAST 5203C(PTB)	39±1	68±4	0.02±0.02	2.08±0.04	2.19	0.26
-	mini CAST F202C/DTD\	C1 1		(870 nm)		(870 nm)	
6	mini-CAST 5203C(PTB)	61±1	102±4	0.06±0.03 (870 nm)	1.73±0.05		0.45
7	mini-CAST 5203C(TROPOS)	99±3	170±5	0.08±0.01	1.28±0.04	5.58	0.62
				(870 nm)		(870 nm)	
8	mini-CAST 5203C(TROPOS)	69±1	116±3	0.04±0.02	1.29±0.05	4.91	0.65
				(870 nm)		(870 nm)	
9	mini-CAST 5203C(TROPOS)	44±3	78±6	0.06±0.02	1.67±0.19	1.75	0.34
				(870 nm)	1	(870 nm)	
10	mini-CAST 5203C(TROPOS)	113±1	194±1	0.08±0.02	1.31±0.03	5.87	
				(870 nm)		(870 nm)	
11	mini-CAST 5203C(TROPOS)	75±1	126±2	0.17±0.08	1.05±0.64	2.54	
12	mini-CAST 5303C	97±1	170.4	(870 nm)	4.42.0.07	(870 nm)	0.76
12	IIIIIII-CAST 3303C	9/11	178±1	0.06±0.01 (870 nm)	1.13±0.07	6.3 (870 nm)	0.76
13	mini-CAST 5303C	67±2	119±3	0.04±0.01	1.13±0.13	7.0	0.66
		07	11525	(870 nm)	1.1320.13	(870 nm)	0.00
14	mini-CAST 5303C	50±2	95±4	0.04±0.01	1.14±0.09	4.41	0.62
				(870 nm)		(870 nm)	
15	FasmaTech spark	-	-	0.27±0.02	0.79±0.06	0.61	0.61
	generator			(870 nm)		(870 nm)	
16	PALAS GFG 1000	171±16	305±32	0.24±0.02	1.64±0.08	4.32	
				(870 nm)	1	(870 nm)	
17	Aquadag	-	325±3	0.26±0	0.31±0.02	7.6	0.6
10	Full areas and	422		(870 nm)	1	(870 nm)	
18	Fullerene soot	122 (bimodal)	356±14	0.40±0.05	0.81±0.05	6.58	
19	Miniature inverted soot	- (billioual)	-	(870 nm)	0.0210.04	(870 nm)	0.54
13	generator		_	0.23±0.01 (870 nm)	0.83±0.04	8.56	0.54
20	Miniature inverted soot	154±10	433±24	0.11±0.01	1.07±0.09	(870 nm) 5.27	
23	generator	13.110	4 55±24	(870 nm)	1.07±0.03	(870 nm)	
21	Miniature inverted soot	249±11	-	0.21±0	0.88±0.04	8.18	0.83
	generator			(870 nm)		(870 nm)	

Figures 4.2 and 4.3 show the results of the correlations of CAPS_{pmssa} and PAX versus CAPS_{pmex}-Aurora4000. Each point represents the average absorption coefficients of a single experiment. Few data are missing because of mismeasurements in single instruments (#4: CAPS_{pmex}-Aurora4000 and #16: PAX).

The linear regression of CAPS_{ssa} and CAPS_{pmex}-Aurora4000 shows excellent agreement between the instruments with a deviation of less than 1% and a coefficient of determination of 0.994. Since both the scattering and extinction channels of CAPS_{pmssa} were calibrated against CAPS_{pmex}-Aurora4000 with PSL particles of sizes 125 nm, 203 nm, and 300 nm, the CAPS_{pmssa} can be considered calibrated against an SI-traceable reference. The good agreement can partly explained by the low single scattering albedos, as uncertainties in measuring the scattering and truncation correction are not significant.

The PAX is lower by an about 10% compared to CAPS_{pmex}-Aurora4000. The deviation is apparently caused by experiments with absorption coefficients in the range of about 200 to 500 Mm⁻¹. A correlation of the deviations with properties such as single scattering albedo and absorption Ångström exponent could not be found. Furthermore, it must be mentioned that the absorption Ångström exponent is determined between 450 and 630 nm and is used for extrapolation to 870 nm. An absolute error of 0.3 in the absorption Ångström exponent can cause a deviation of 10%. It should be noted that Ångström exponents are not constant over the broad spectral range and should therefore be used with caution for extrapolation. Whether the deviation is an artefact of the special calibration with aerosols cannot be determined at present. Taking all these uncertainties into account, a clarification does not seem possible without further dedicated experiments.

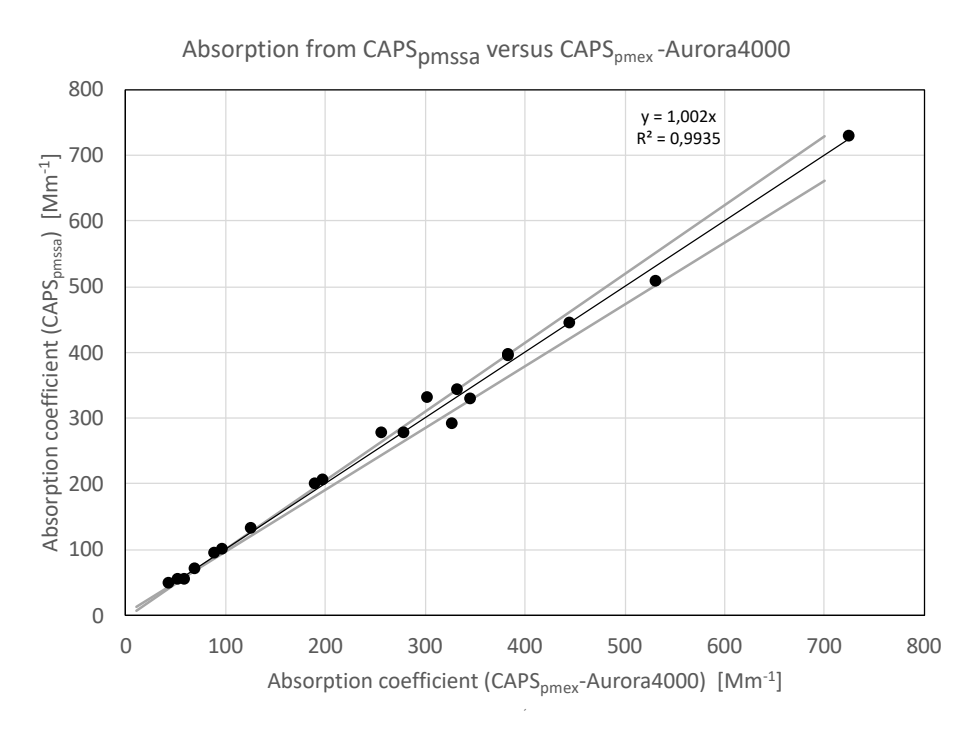


Figure 4.2: Absorption from CAPS_{pmssa} versus CAPS_{pmex}-Aurora4000. The points represent single experiments from Table 1. The black line is the linear regression line for both methods and the grey lines indicates the ±5% uncertainty range of CAPS_{pmex}-Aurora4000.

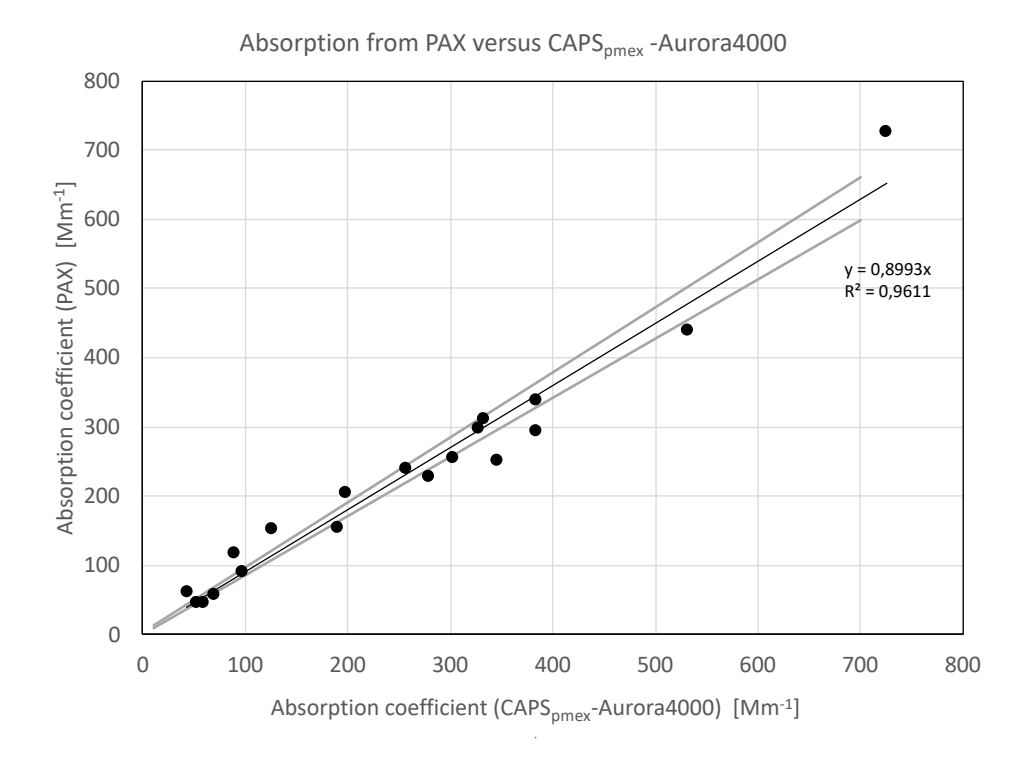


Figure 4.3: Absorption from PAX versus CAPS_{pmex}-Aurora4000. The points represent single experiments from Table 1. The black line is the linear regression line for both methods and the grey lines indicates the $\pm 5\%$ uncertainty range of CAPS_{pmex}-Aurora4000.

AEROTOX campaign

The AeroTox campaign took place at MEATS (Switzerland) in September 2020. The aim of this experiment was to investigated the physical properties of different black carbon aerosols with and without coating. During this experiment, the MSPTI, a MAAP and a PAX were also used. This experiment is the first experiment in which the light absorption coefficients of MSPTI were compared to other techniques. The data is still being processed, therefore the results are preliminary.

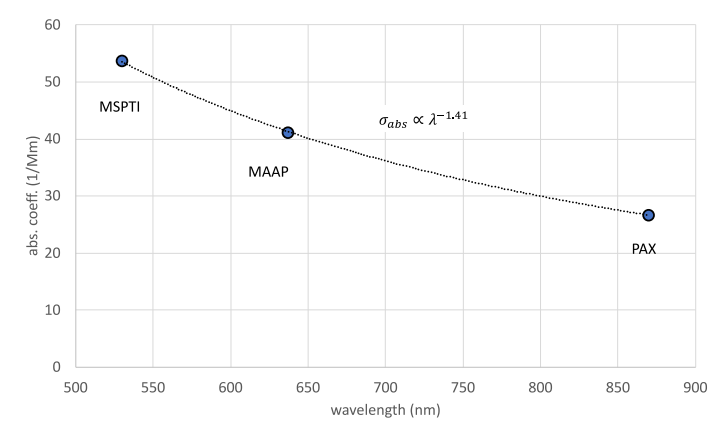


Figure 4.3: Spectral absorption measured with MSPTI at 532 nm, MAAP at 637 nm and PAX at 870 nm.

For one experiment, Figure 4.3 shows the calculated spectral absorption measured with MSPTI, MAAP and PAX. The spectral response shows an absorption Ångström exponent (AAE) of 1.41. In contrast, with AE33 an AAE of 1.21 was measured. The AE33 data were not integrated into the plot because the multiple scattering parameter needed for calculating the absorption coefficient is strongly size dependent, as shown in deliverable D4 (Figure 13). In order to assess the uncertainties of the measurements, and also the differences in the absorption Ångström coefficient, the data from this campaign must first be fully evaluated.

5. Summary of results

This chapter summarizes the results and harmonizes information from the chapters on the individual instruments.

Si traceability and calibration:

SI-traceable calibration is in all cases based on a calibration using gases, either the measurement of the light absorption in an absorption band (MSPTI) or the measurement of the Rayleigh light scattering coefficient in the CAPS_{pmex}-Aurora4000 setup. Therefore, only MSPTI and Extinction minus scattering based on CAPS_{pmex}-Aurora4000 are SI-traceable methods.

Both EMS methods (CAPS_{pmex}-Aurora4000 and CAPS_{ssa}) perform a cross calibration using suitable non-absorbing aerosols. It is advantageous to have combined measuring cells (CAPS_{ssa}) for measuring scattering and extinction to avoid bias due to particle losses. The PAX performs a calibration of the light absorption by an extinction measurement with a sufficiently low single scattering albedo.

SI-traceable method could be considered as primary standards as the calibration is reproduceable in any laboratory using certified gases. CAPS_{pmssa} and PAX could instead be considered as secondary standards since these methods can be calibrated using primary methods. Furthermore, cross calibration between scattering and extinction (aerosol with high single scattering albedo) for CAPS_{ssa} and extinction and absorption (aerosol with low single scattering albedo) for PAX using aerosols can confirm the validity of the calibration, allowing these instruments to be used as a field reference.

Portability:

For field applications it is important to discuss portability and subsequent actions to calibrate the setup or confirm calibration.

For CAPS_{pmex}-Aurora4000, a setup of multiple instruments has to be transported. Even if care is taken to rebuild the setup including the aerosol tube in its original configuration, recalibration is strongly recommended. For CAPS_{pmssa} it could be confirmed by cross calibration that the calibration of the scattering and extinction channels have not changed against each other. MSPTI instruments require realignment of optics and recalibration, what limits the portability. For PAX, a calibration check after transport would be desirable. According to the user manual (Droplet Measurement Technologies, 2018), this could be done with a simple apparatus for measuring flame soot. Since the simple structure of the soot is not known a priori, this method can only be carried out with a larger degree of uncertainty.

Frequency of calibrations and baseline measurements

The frequency of calibrations was not investigated in details for all setup. For MSPTI, the long term long stability of the calibration could not be investigated due to time constraints. The baseline in MSPTI is measure continuously. For CAPS_{pmex}-Aurora4000, the stability of the calibration was found to be good for periods of a couple of months and the frequency of baseline measurements should be between 5 minutes and 15 minutes. For CAPS_{ssa} no specific measurements were done. It can be argued that the performance is similar to the CAPS_{pmex}-Aurora4000 setup.

Relative uncertainty and detection limit of absorption coefficients

For comparability of the accuracy of the derived absorption coefficients, the following scenarios are investigated:

- The instruments are equipped with a pre-impactor to avoid large truncation correction errors. For a focus of aerosols whose absorption coefficient is dominated by soot, this is not a significant limitation.
- Aerosols with extinction coefficients of 10 Mm⁻¹ and 100 Mm⁻¹ and single scattering albedos of 0.8 and smaller 0.2 are considered.
- Uncertainties are given for two minutes averages.

Relative uncertainties for EMS (CAPS_{pmex}-Aurora4000) were calculated using the error propagation scheme shown in chapter 3. Relative uncertainties for EMS (CAPS_{pmssa}) were taken from Modini et al. (2021) (c.f. Figure 3.2.4 in this report). The relative error for MSPTI cannot be given because the new design has just been developed and not enough independent calibration has been performed. Also, due to the limitations of COVID19, no comparison with EMS (CAPS_{pmex}-Aurora4000) could be performed yet.

The detection limit of EMS (CAPS_{pmex}-Aurora4000) is dominated by the baseline drift of CAPS_{pmex}. The detection limits for two minutes averaging time 1.29 Mm⁻¹ (450 nm), 0.98 Mm⁻¹ (525 nm) and 1.14 Mm⁻¹ (635 nm). The CAPS_{ssa} detection limit has not yet been determined. It can be argued that with similar noise of the extinction and scatter measurements, the baseline drift also dominates the uncertainty. The value is therefore estimated to be about 1.0 Mm⁻¹.

The detection limit of MSPTI was determined to be 0.4 $\rm Mm^{-1}$ (1 σ noise) for NO₂. Because of statistical noise due the low number of particles, the detection limit for particles is about a factor of two higher. In total, the 1 σ detection limit is about 1.6 $\rm Mm^{-1}$.

The detection limit for the absorption coefficient for PAX was calculated to be 0.33 Mm⁻¹. It should be noted, that this value is based on the instrumental noise and does not include uncertainties of baseline measurements. The expected relative error can not be estimated but was determined by intercomparison measurement a primary method, the CAPS_{pmex}-Aurora4000. The deviation of between the system was found to be about 10%. With the available measurements, it cannot be estimated whether there are dependencies on the single scattering albedo or on the level of the absorption coefficient.

Multiwavelength measurements

The number of wavelengths in the EMS CAPS_{pmex}-Aurora4000 combination is realized through a three wavelength Nephelometer and three single wavelength CAPS_{pmex}. As shown in chapter 3.1, a covariance between few calibration constants of the nephelometer and CAPS_{pmex} occurs. Therefore, the entire system cannot theoretically be considered a reference system with three fully independent wavelengths.

For CAPS_{ssa}, it is in principle possible to combine several units of different wavelengths into a multi-wavelength setup. Although not carried out in this project, it can be concluded that a cross calibration or comparison with a multi-wavelength nephelometer should be carried out for all instruments at the same time so that changes in ambient conditions or test aerosols or gases do not cause a bias in the spectral response.

For nephelometers, CAPS_{pmex} and CAPS_{pmssa} no specific wavelengths are required for calibration and cross calibration with Rayleigh scattering gases and light scattering aerosols. However, both types of CAPS instruments require a measurement cell adopted to the wavelength because of the required high mirror reflectivity.

With MSPTI, a suitable combination of laser and calibration gas must be used for other wavelengths. An extension to a multi-wavelength setup therefore requires a high development effort and possibly also several calibration gases.

Since PAX is not calibrated with a gas like other photacoustic absorption photometers, but with aerosols, the technique can therefore be adapted to other wavelengths.

Cross sensitivity to absorbing gases:

The cross sensitivity to absorbing gases was subject of deliverable D1 (Fig. 2 in D2).

Compensation of absorption by gases is done by baseline measurements with filtered air. As already mentioned, limitations of the compensation must be expected due to a time-delayed adsorption and release of the gases through the filter.

With CAPS_{pmex}-Aurora4000, CAPS_{pmssa} and PAX, the regular measurements and zero measurements are carried out consecutively, so that a high temporal variability of the gases can cause further uncertainties. With the MSPTI, this is avoided by a simultaneous reference measurement.

Inlet and aerosol transportation losses:

To avoid trasnport losses, the aerosol lines should be kept as short as possible, and in the case of EMS (CAPS_{pmex}-Aurora4000) should be kept as equal as possible. However, since the focus is on soot particles in the submicrometer range, no significant losses are to be expected. To keep the influence of coarse mode particles in the truncation correction of the light scattering measurement of the two EMS methods small, a PM1 impactor is recommended.

Table 5.1: Summary of properties of the systems under investigation.

Method		Extinction minus	Scattering	Photothermal Interferometry	Photoacustic
Instruments		CAPS _{pmex} -Aurora4000	CAPS _{ssa}	MSPTI	PAX
Wavelengths		450nm, 525 nm, 635 nm	630 nm, 780 nm	532 nm	870 nm
Detection limit (2σ noise, 2 minutes avg. time)		1.29 Mm ⁻¹ (450 nm) 0.98 Mm ⁻¹ (525 nm)			
		1.14 Mm ⁻¹ (635 nm)	Approx. 1 Mm ⁻¹	Approx. 1.6 Mm ⁻¹	0.33 Mm ⁻¹
Relative error of	ssa=0.2, b _{ext} =100 Mm ⁻¹	5%		Not specified	10 %
absorption coefficient	ssa=0.2, b _{ext} =10 Mm ⁻¹	9%	9%		10%
	ssa=0.8, b _{ext} =100 Mm ⁻¹	8%	20%		10%
	ssa=0.8, b _{ext} =10 Mm ⁻¹	41%	30%		10%
Frequency of baseline measurements		Neph. baseline every 24h CAPS _{pmex} baseline every 5 min	CAPS _{pmssa} baseline every 5 min	Continuously	15 minutes
Long term stability of calibration		Several months	Not specified	Not specified	Not specified
Calibration method		Gas calibration of sca. and cross calibration between ext. and sca.	Cross calibration between ext. and sca.	Gas absorption	Calibration of scattering and absorption channels using particles
Si-traceability		Yes	No	Yes	No
Cross sensitivity to absorbing gases		Yes	Yes	No	yes
Portability		Yes with some efforts.	Yes.	Yes.	Yes
		Recalibration required.	Cross calibration recommended	Requires alignment of optics and recalibration	
Requirements for full calibration		High and low span gas (e.g. CO2 and air) Scattering aerosol for cross calibration	Scattering aerosol for cross calibration	Calibration gas (NO ₂)	Soot and non- absorbing particles with very high concentrations

In summary, two potential Si-traceable primary methods could be identified. These are the well-known extinction minus scattering method, based on a combination of nephelometer and extinction cell, and the not yet widely used PTI techniques. Due to limitations in portability, these setups are not well suited as field references in the current state of development. Two other setups are secondary standards, as direct calibration to SI units is lacking. However, these units are better suited as field references.

All methods are subject to the high detection limit when compared with typical values of the absorption coefficient for ambient air. In addition, the EMS methods have higher uncertainties at high single scattering albedos. Therefore, field calibration of filter-based absorption photometers with ambient air is only possible in rare cases. However, with a transportable black carbon generator to produce black carbon particles with reproducible properties, field calibrations would be feasible and would also reduce the uncertainties due to gas absorption. It should be noted that such a black carbon generator would also support cross-calibration of PAX in the field

In this compilation, no classical photoacoustic photometer has been considered, where the calibration is performed with absorbing gases. According to the criteria applied here, such a device would be considered as a primary standard.

6. References

Anderson, T. L., et al. (1996). "Performance characteristics of a high-sensitivity, three-wavelength, total scatter/backscatter nephelometer." Journal of Atmospheric and Oceanic Technology 13(5): 967-986.

Anderson, T. L. and J. A. Ogren (1998). "Determining aerosol radiative properties using the TSI 3563 integrating nephelometer." Aerosol Science and Technology 29(1): 57-69.

Arnott, P. et al. (1999). "Photoacoustic spectrometer for measuring light absorption by aerosol: instrument description". Atmos. Environ. 33, 2845–2852 (1999).

Bond, T. C., et al. (1999). "Calibration and intercomparison of filter-based measurements of visible light absorption by aerosols." Aerosol Science and Technology 30(6): 582-600.

Droplet Measurement Technologies (2018). "Photoacoustic Extinctiometer (PAX). Operator Manual DOC-0301 Revision E." Longmont, USA.

Lack, D. A., et al. (2006). "Absorption Measurement using Photoacoustic Spectroscopy: Sensitivity, Calibration, and Uncertainty Developments." Aerosol Sci. Technol. 40, 697–708.

Lee, J., and Moosmüller, H. (2020). "Measurement of Light Absorbing Aerosols with Folded-Jamin Photothermal Interferometry", Sensors (Basel), 20, 10.3390/s20092615.

Lewis, K. et al. (2008). "Strong spectral variation of biomass smoke light absorption and single scattering albedo observed with a novel dual-wavelength photoacoustic instrument." J. Geophys. Res. 113, D16203.

Massoli, P. et al. (2010). "Aerosol Light Extinction Measurements by Cavity Attenuated Phase Shift (CAPS) Spectroscopy: Laboratory Validation and Field Deployment of a Compact Aerosol Particle Extinction Monitor", Aerosol Science and Technology, 44(6), 428–435, doi:10.1080/02786821003716599.

Modini, R. L. et al. (2021), "Detailed characterization of the CAPS single scattering albedo monitor (CAPS PMssa) as a field-deployable instrument for measuring aerosol light absorption with the extinction-minus-scattering method", Atmos. Meas. Tech. Discuss., https://doi.org/10.5194/amt-2020-292 [in press].

Moosmüller, H., et al. (2009). "Aerosol light absorption and its measurement: A review." Journal of Quantitative Spectroscopy and Radiative Transfer 110(11): 844-878.

Müller, T., et al. (2011). "Design and performance of a three-wavelength LED-based total scatter and backscatter integrating nephelometer." Atmospheric Measurement Techniques 4: 1291-1303.

Nakayama, T. et al. (2015). "Characterization of a Three Wavelength Photoacoustic Soot Spectrometer (PASS-3) and a Photoacoustic Extinctiometer (PAX)." J. Meteorol. Soc. Japan. Ser. II 93, 285–308.

Onasch, T. B., et al. (2015). "Single Scattering Albedo Monitor for Airborne Particulates." Aerosol Science and Technology 49(4): 267-279.

Petzold, A. and Niessner, R. (1995). "Novel design of a resonant photoacoustic spectrophone for elemental carbon mass monitoring." Appl. Phys. Lett. 66, 1285–1287.

Petzold, A., et al. (2013). "Intercomparison of a Cavity Attenuated Phase Shift-based extinction monitor (CAPS PMex) with an integrating nephelometer and a filter-based absorption monitor." Atmospheric Measurement Techniques 6(5): 1141-1151.

Pfeifer, S., et al. (2020). "The influence of the baseline drift on the resulting extinction values of a cavity attenuated phase shift-based extinction monitor (CAPS PMex)." Atmospheric Measurement Techniques 13: 2161–2167.

Schnaiter, M., et al. (2005). "Measurement of wavelength-resolved light absorption by aerosols utilizing a UV-VIS extinction cell." Aerosol Science and Technology 39(3): 249-260.

Sedlacek, A., and Lee, J. (2007). "Photothermal interferometric aerosol absorption spectrometry." Aerosol Sci. Technol., 41, 1089-1101, 10.1080/02786820701697812.

Sheridan, P. J., et al. (2005). "The Reno Aerosol Optics Study: An evaluation of aerosol absorption measurement methods." Aerosol Science and Technology 39(1): 1-16.

Visser, B., et al. (2020). "A single-beam photothermal interferometer for in-situ measurements of aerosol light absorption." Atmos. Meas. Tech., 13, 7097–7111, 2020https://doi.org/10.5194/amt-13-7097-2020.